FCTUC FACULDADE DE CIÊNCIAS E TECNOLOGIA
UNIVERSIDADE DE COIMBRA

Carlos Filipe Gonçalves Moreira

Inhibiting COMT in a mouse model of Parkinson's disease: a trial of Tolcapone in VMAT2-deficient mice

Dissertation presented to the University of Coimbra in fulfillment of the requirements necessary for obtaining a MSc degree in Biomedical Engineering

Supervisors:

Dr. sci. nat. Daniela Noain[1]

Prof. Dr. João Oliveira Malva[2]

[1]Neurology Department, University Hospital of Zurich (USZ), Switzerland

[2]Faculty of Medicine of the University of Coimbra (FMUC), Portugal

Coimbra, 2015

This project was developed in collaboration with:

Neurology Department, University Hospital of Zurich (USZ), Switzerland

ACKNOWLEDGEMENTS

First, I have to thank everyone who are part of the Animal Sleep Laboratory at the University Hospital of Zürich: I owe special appreciation to Dr. Daniela Noain and Dr. Christian Baumann, for accepting my application and for always being by my side during this project.
Many profound thanks also to Dr. Sophie Masneuf, Marta Morawska, Aron Baumann, Raquel Machado, Ana Telma Santos, Fabian Preisig, and many others for all the help and knowledge they shared with me. I am grateful for this unforgettable year.
I also owe special gratitude to Dr. João Oliveira Malva for being available as home-institution supervisor.

Dedico este trabalho aos meus amigos. Obrigado por fazerem da distância um detalhe sem significado.

Por último, obrigado aos meus pais e irmão.
Tudo o que sou, devo-vos a vós!

RESUMO

Na doença de Parkinson, a perda progressiva de neurónios produtores de dopamina da substantia nigra pars compacta conduz a desequilíbrios neuroquímicos da gânglia basal e, consequentemente, ao surgimento de sintomas como bradicinesia, rigidez das extremidades e tremor. Sintomas reminiscentes destas disfunções motoras, assim como sinais não motores de doença de Parkinson, foram revelados num modelo transgénico de murganho, modelo este que expressa apenas 5% da proteína transportadora vesicular monoaminérgica (VMAT2-deficient). A doença de Parkinson é tipicamente tratada com o fármaco L-DOPA, um percursor da dopamina. Dado que a degradação da molécula de L-DOPA pela enzima catecol-O-metiltransferase (COMT) leva ao aumento dos níveis de homocisteína, um fator de risco cardiovascular e demência, a reposição terapêutica prolongada de dopamina poderá acelerar a disfunção neuronal e a neurodegeneração. Para além do uso de L-DOPA, tentativas anteriores para restaurar os níveis de dopamina e simultaneamente promoverem neuroprotecção não foram bem-sucedidas. Este estudo investigará os efeitos do inibidor enzimático da enzima COMT, Tolcapone, nas funções motoras, nas performances olfactiva e cognitiva, e mais tarde, na evolução dos marcadores bioquímicos de neurodegeneração e dos níveis sanguíneos de homocisteína em murganhos VMAT2-deficient. Propõe-se que o fármaco Tolcapone possa não só reduzir a degradação de L-DOPA mas adicionalmente favorecer o tratamento da doença de Parkinson aumentando e estabilizando os níveis de dopamina. Além disso, sugere-se ainda que a inibição farmacológica da enzima COMT oferece benefícios significativos a longo-prazo no contexto da doença de Parkinson: reduz o risco de episódios cardiovasculares, atrasa o aparecimento de declínio cognitivo, e sobretudo, oferece significativos efeitos neuroprotetores.

Palavras-chave: doença de Parkinson, inibição de COMT, neurofarmacologia, modelo animal de PD, comportamento.

ABSTRACT

In patients with Parkinson's disease, the progressive loss of dopamine-producing cells in the substantia nigra pars compacta leads to a neurochemical imbalance in the basal ganglia and finally to bradykinesia, rigidity and tremor. Symptoms reminiscent of these motor dysfunctions, as well as of non-motor signs of Parkinson's disease, were revealed in transgenic mice with 5% expression of vesicular monoamine transporter 2 (VMAT2-deficient mice). PD is typically treated with dopaminergic drugs, in particular L-DOPA. Because methylation of L-DOPA by catechol-O-methyltransferase (COMT) leads to increased concentration of homocysteine, which is a known risk factor of vascular events and cognitive impairment, dopamine replacement may accelerate neuronal dysfunction and neurodegeneration. Previous attempts to restore striatal dopamine apart from L-DOPA and provide neuroprotection remained unsuccessful. As a novel approach, this study proposes to investigate the effects of the COMT inhibitor, Tolcapone, on motor function, olfactory and cognitive performances, and later, on biochemical markers of neurodegeneration and marker substances of homocysteine metabolism in peripheral blood in VMAT2-deficient mice. It is hypothesized that Tolcapone may not only inhibit the degradation of L-DOPA but further improve PD treatment by increasing and stabilizing serum dopamine concentrations, and ultimately, show in prospective manner whether pharmacological inhibition of COMT offers significant benefit in Parkinson's disease context by reducing risk of vascular events and cognitive decline, and exerts neuroprotective effect.

Key words: Parkinson's disease, COMT inhibition, neuropharmacology, PD mouse model, behaviour.

ABBREVIATIONS

$^{\bullet}$OH, hydroxyl
3-MT, 3-methoxytyramine
3-OMD, 3-methoxy-4-hydroxy-L-phenylalanine
5-HT, serotonin
6-OHDA, 6-hydroxydopamine
AADC, acid decarboxylase
ADP, adenosine diphosphate
ALT, glutamic pyruvic transaminase/alanine aminotransferase
AST, glutamic-oxaloacetic transaminase/aspartate aminotransferase
ATP, adenosine triphosphate
ATPase, adenosine triphosphatase
BBB, blood-brain barrier
CNS, central nervous system
COMT, catechol-O-methyltransferase
DA, dopamine
DAT, dopamine transporter
DBS, deep brain stimulation
DOPAC, 3,4-dihydroxyphenylacetate
DOPAL, 3,4-dihydroxyphenylacetaldehyde
DR, dopamine receptor
GI, gastrointestinal
H_2O_2, hydrogen peroxide
Hcy, homocysteine
HHcy, hyperhomocysteinemia
HVA, homovanillic acid
LB, Lewy bodies
LC, locus coeruleus
L-DOPA, l-dihydroxylphenylalanine
LRRK2, leucine-rich repeat kinase 2
MAO, monoamine oxidase

MB-COMT, membrane-bound catechol-O-methyltransferase
MPTP, 1-methyl-4-phenyl-1,2,3,6-tetrahydropyridine
NE, norepinephrine
NH_3, ammonia
$O_2^{\bullet-}$, superoxide
PD, Parkinson's disease
PFC, prefrontal cortex
P_i, inorganic phosphate
PRKN, parkin
REM, rapid eye movement
ROS, reactive oxygen species
SAH, S-adenosyl-L-homocysteine
SAM, S-adenosyl-L-methionine
S-COMT, soluble catechol-O-methyltransferase
SNpc, substantia nigra pars compact
TH, tyrosine hydroxylase
tHcy, total homocysteine
Tyr, tyrosine
UPS, ubiquitin-proteasome system
USZ, University Hospital of Zurich
VMAT2 LO, expressing only 5% of the VMAT2
VMAT2 WT, wild-type animal
VMAT2, vesicular monoamine transporter-2
VTA, ventral tegmental area

INDEX

CHAPTER 1

INTRODUCTION

1.1. DOPAMINE FUNCTIONS AND METABOLISM

Dopamine (DA) is a hormone and one of the primary catecholamine neurotransmitters present in the mammalian brain. The study of catecholamine neurons started in the 1960s, when Carlsson, Falck and Hillarp used new methods to first describe norepinephrine (NE) and DA in discrete neuronal systems (Carlsson et al., 1964; Falck et al., 1982).

The amino acid tyrosine (Tyr) is the precursor of DA and undergoes hydroxylation into l-dihydroxyphenylalanine (L-DOPA), a reaction catalyzed in the cytosol by the rate-limiting enzyme tyrosine hydroxylase (TH) together with molecular oxygen (O_2), ferrous iron (Fe^{2+}) and tetrahydrobiopterin (BH_4) as cofactors. Afterwards, L-DOPA is decarboxylated into DA, a conversion catalyzed by the aromatic amino acid decarboxylase (AADC) and the cofactor pyridoxal phosphate that generates carbon dioxide (CO_2) (Daubner et al., 2011).

DA activity underlies multiple brain functions including locomotor activity, food intake, cognition, motivation, positive reinforcement and endocrine regulation, as well as it is also involved in the peripheral system as a modulator of both cardiovascular and renal functions, gastrointestinal motility (GI), hormone secretion, and vascular tone (Missale et al., 1998).

The dopaminergic neurons synthesize, store and release DA to the synaptic space. They are confined to several small brain areas, primarily the ventral tegmental area (VTA) and the substantia nigra (SN), from where they extend axonal projections to distal brain regions, such as the striatum, the limbic system and the prefrontal cortex (PFC) (Björklund and Dunnett, 2007).

1.1.1. VESICULAR MONOAMINE TRANSPORTER 2

Associated with TH and AADC is the vesicular monoamine transporter-2 (VMAT2), a 12-transmembrane domain proton-pumping adenosine triphosphatase (H^+-ATPase) antiporter that transports DA synthesized in the cytosol (or recycled from the extracellular space) into small synaptic and dense core vesicles (Figure 1.1). Together they assemble a complex (TH-AADC-VMAT2) that converts Tyr to L-DOPA and L-DOPA to DA. Then, DA is taken up into vesicles (Cartier et al., 2009), preventing its spontaneous oxidation at physiological *pH* (*pH* 7.4) to neurotoxic DA-O-quinone, superoxide radicals ($O_2^{\cdot -}$) and hydrogen peroxide (H_2O_2). H_2O_2 is precursor of cytotoxic hydroxyl radicals ($^{\cdot -}OH$), catalyzed by copper (Cu^+) or Fe^{2+}, found in particular high concentrations in the SN pars compacta (SNpc) than in other brain regions.

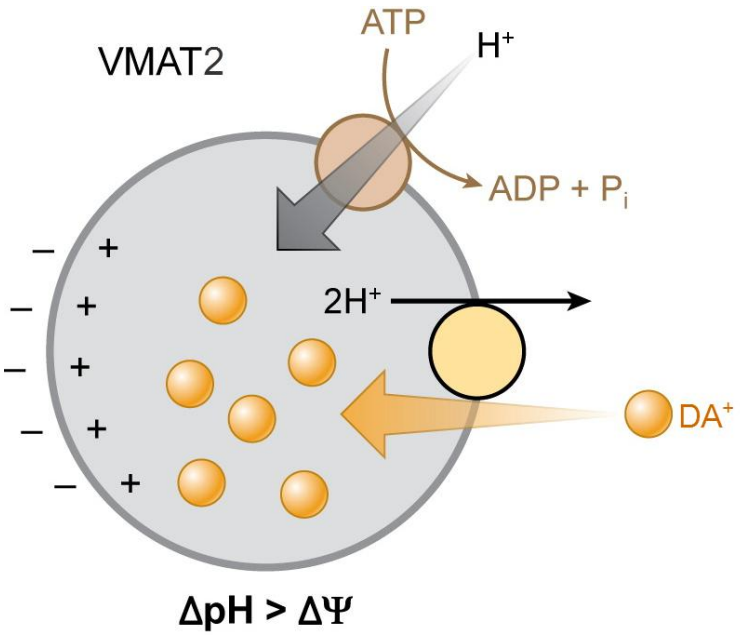

Figure 1.1 – Cytosolic DA sequestration dependent on VMAT2 transporter. The intrasynaptic vesicle contain an ATPase that hydrolyzes ATP to ADP and P_i, translocating one proton (H^+) into the vesicle and triggering a proton gradient. VMAT2 uses this proton gradient across the vesicular membrane as the driving force to take up one positively charged molecule of DA with the concomitant release of two H^+. (ADP: adenosine diphosphate; ATP: adenosine triphosphate; ATPase: adenosine triphosphatase; P_i: inorganic phosphate; VMAT2: vesicular monoamine transporter-2). Modified from Chaudhry and colleagues (Chaudhry et al., 2008**).**

The increase of H^+ inside these vesicles induces a decrease in the *pH* at the inner environment, which is estimated to be 2 to 2.4 *pH* units lower than that of the cytosol (Guillot and Miller, 2009) preventing the protons of the DA hydroxyl groups to dissociate from the oxygen.

Later on, soluble NSF attachment receptors (SNARES) and a series of protein complexes drive the DA-loaded vesicle to the plasma membrane, perform the docking and prime the vesicle for membrane fusion and exocytotic release (Li and Chin, 2003). Thus, VMAT2 is a crucial intracellular regulator of both the size of the vesicular DA pool and the availability of DA in the cytosol. In addition, VMAT2 is liable for interacting with several exogenous and endogenous toxins that appear to gain access to the dopaminergic neuron and ultimately impact its function and survival. VMAT2 is present all through the central nervous system (CNS), where it is also responsible for regulating and packaging serotonin (5-HT), NE, epinephrine and histamine in their respective neuronal systems (Erickson et al., 1996), and in the periphery in mast cells and platelets.

1.1.2. DA DYNAMICS: DAT, MAO AND COMT

The balance between the quantity of DA released, the duration of effects, and the responsiveness of postsynaptic receptors is crucial for the DA signaling dynamics. DA transporter (DAT), an exclusive symporter of dopaminergic neurons and member of the sodium/chloride-coupled (Na^+/Cl^-) neurotransmitter transporter family, plays an important part in regulating the duration of action of DA in the extracellular space, as well as in maintaining the delicate stability between DA synthesis, release, recycling and degradation (Jones et al., 1997) (Figure 1.2). This way, inhibition of DAT reduces DA reuptake and consequently increases its extracellular and synaptic concentrations as well as its lifespan, which leads to a prolonged stimulation of both postsynaptic and presynaptic DA receptors (D1-D5) (Kuhar, 1992).

Monoamine oxidase (MAO) is a mitochondrial outer membrane-bound flavoenzyme found in neurons and glia cells. It catalyzes the oxidative deamination of the cytosolic DA amino group to 3,4-

dihydroxyphenylacetaldehyde (DOPAL, non-toxic metabolite) along with formation of ammonia (NH_3) and H_2O_2. DOPAL is further oxidized by aldehyde dehydrogenase (AD) to non-toxic 3,4-dihydroxyphenylacetate (DOPAC) (Binda et al., 2011), which can be further converted to homovanillic acid (HVA) catalyzed by catechol-O-methyltransferase (COMT).

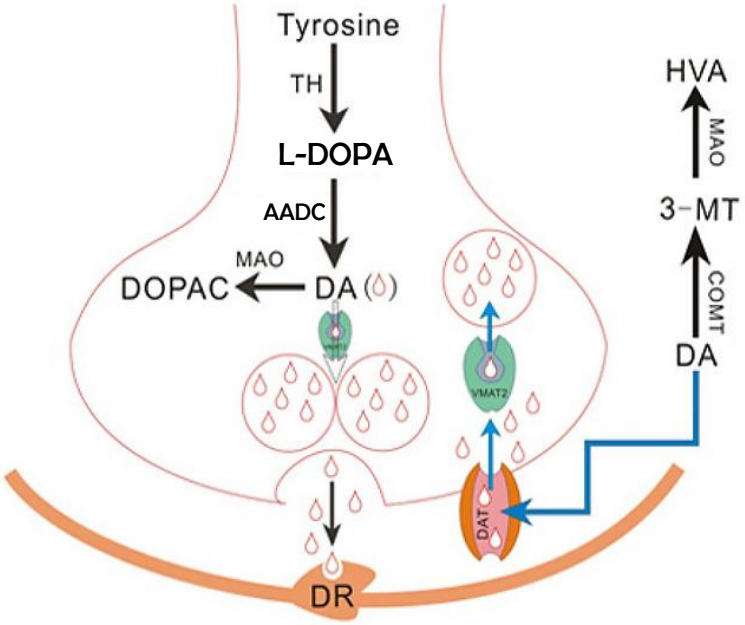

Figure 1.2 – DA sequestration, release, reuptake and breakdown. The DA present in the synaptic cleft is co-transported with two sodium ions (Na^+) and one chloride ion (Cl^-) into presynaptic terminals, as a result of the ion concentration gradient that is generated by the plasma membrane sodium-potassium adenosine triphosphatase (Na^+/K^+-ATPase). This recycled DA constitutes also a source of free cytosolic DA and can be sequestered again in monoaminergic vesicles. DA that was not immediately packaged inside presynaptic neurons is taken up by surrounding glial cells and gets degraded by COMT and MAO enzymes. (3-MT: 3-methoxytyramine; AADC: aromatic amino acid decarboxylase; DAT: DA trasporter; DOPAC: 3,4-dihydroxyphenylacetate; DR: DA receptor; COMT: catechol-O-methyltransferase; HVA: homovanillic acid; MAO: monoamine oxidase; TH: tyrosine hydroxylase). Modified from Sun and colleagues (Sun et al., 2014).

COMT is a magnesium-dependent intracellular enzyme discovered by Axelrod and coworkers (Axelrod and Tomchick, 1958) present both in the brain and in the periphery, mainly the liver. It catalyzes the methylation of catechol substrates (for instance L-DOPA) using S-adenosyl-L-methionine (SAM) as a methyl donor, resulting O-methylated catechol (such as 3-methoxy-4-hydroxy-L-phenylalanine [3-OMD], from L-DOPA) and S-adenosyl-L-homocysteine (SAH) as reaction products. When DA floods into

the synaptic space and does not bind to receptors or is not taken back into the neuron via DAT, it gets degraded into 3-methoxytyramine (3-MT) by COMT and further metabolized by MAO to HVA (Figure 1.3).

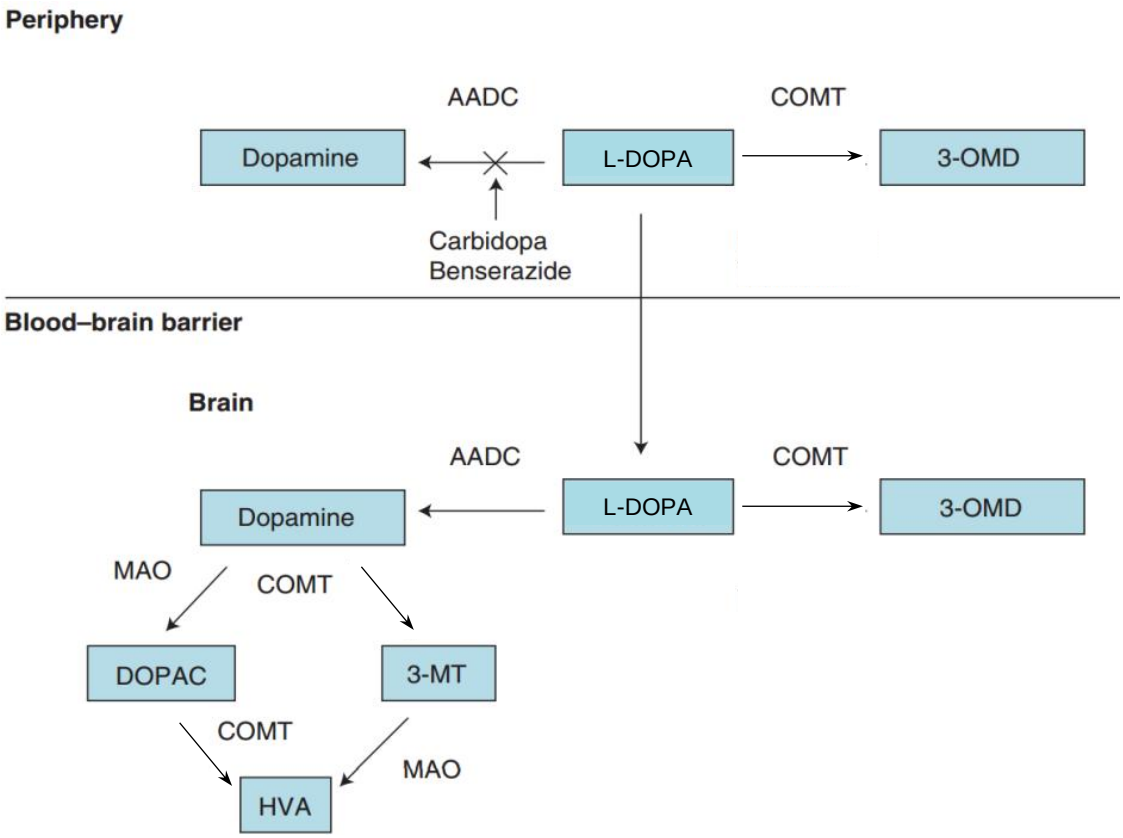

Figure 1.3 – Metabolism of L-DOPA. (AADC: aromatic amino acid decarboxylase; COMT: catechol-O-methyltransferase; DOPAC: 3,4-dihydroxyphenylacetic acid; HVA: homovanillic acid; MAO: monoamine oxidase; 3-MT: 3-methoxytyramine; 3-OMD: 3-O-methyldopa). Modified from Leegwater-Kim and Waters, (Leegwater-Kim and Waters, 2006).

Human COMT is present in two distinct isoforms: membrane-bound (MB-COMT), which is the predominantly expressed form in the mammalian CNS and it is localized in the rough endoplasmic reticulum, and soluble (S-COMT), found primarily in the cytoplasm of glial cells and peripheral tissues, such as the liver. Although MB-COMT and S-COMT share similar affinities for SAM, they have significantly different affinities for substrates such as DA (Espinoza et al., 2012).

Degradation of DA by COMT might be a key process in the regulation of its availability at certain brain sites, such as the prefrontal cortex (PFC),

where DAT low expression within synapses turns DA uptake slower (Wayment et al., 2001) compared to the striatum, where it is able to terminate the synaptic action of DA by rapid neuronal uptake (Giros et al., 1996).

1.1.3. DOPAMINE DYSREGULATION

DA imbalances and dysregulation of dopaminergic neurotransmission are linked to several neuropsychiatric and neurological conditions such as Parkinson's disease (PD), schizophrenia, Tourette's syndrome, attention-deficit with hyperactivity disorder, and drug addiction, among others. Indeed, DA is inherently neurotoxic either by auto-oxidation or enzymatic metabolism. The generation of reactive oxygen species (ROS) from cytosolic DA, likely in combination with other factors such as mitochondrial dysfunction, α-synuclein aggregation, neuroinflammation, and impaired protein degradation lead to functional modifications in proteins, DNA and lipids. Lipid damage, in turn, compromises membrane integrity and increases permeability to ions like calcium (Ca^{2+}), promoting excitotoxicity. Thus, VMAT2 is determinant in DA clearance and the reduction in its expression or its loss of function could adversely affect DA vesicular sequestration, a concomitant accumulation of cytosolic DA easily oxidizable and its depletion in the striatum, and development of a parkinsonian phenotype (Caudle et al., 2007).

1.2. PARKINSON'S DISEASE

James Parkinson first described in his 1817 famous monograph '*An essay for the Shaking Palsy*', some of the characteristics of the disorder named after him today. Parkinson described an apparent neurological illness based on just six individuals with a clear progressive motor disability (Parkinson, 1817; re-edition 2002). However, only in 1960, Ehringer and Hornykiewicz uncovered the signs of decreased DA concentration in the striatum of patients with PD (Ehringer and Hornykiewicz, 1962). This discovery enabled the first trials of L-DOPA in PD patients (Birkmayer and Hornykiewicz, 1998). More recently, some aspects contributing to death of

dopaminergic and non-dopaminergic cells in patients with PD have been identified, such as genetic mutations, anomalous processing of misfolded proteins by the ubiquitin-proteasome system (UPS) and the autophagy-lysosomal mechanism, increased oxidative stress, mitochondrial dysfunction, inflammation and other processes (McNaught et al., 2001; Jankovic, 2008; Pan et al., 2008).

Worldwide, this late-onset, slowly progressive synucleinopathy is the second most common neurodegenerative disorder after Alzheimer's disease and the most common movement disorder, affecting 1-2% of the population aged over 65 and nearly 5% by age 85 (Di Giovanni et al., 2010).

1.2.1. PATHOPHYSIOLOGY

PD is characterized by severe motor disturbances, including resting tremor, postural instability, bradykinesia and progressive rigidity. Likewise, festinating gait, lack of facial expression, and eye blinking are often observed. The pathophysiological changes are extensive and marked by the death of neuromelanin-containing DA neurons in the SNpc, which results in a drastic reduction of dopaminergic projections to the striatum. Due to the major loss of striatal innervation, compensatory adjustments occur in DA dynamics, including increased DA synthesis and release in the remaining neurons, and up-regulation of postsynaptic DA receptors. However, in PD patients already exhibiting motor dysfunctions, these adaptations do not appear sufficient to counterbalance the loss of more than 50% of dopaminergic neurons projecting from the SNpc to the striatum and approximately 80% reduction in striatal DA levels (Fearnley and Lees, 1991). Moreover, additional neuronal systems are also affected, although less acutely, evidenced by degeneration of NE neurons of the locus coeruleus (LC), 5-HT neurons of the raphe nuclei, the dorsal motor nucleus of the vagus nerve, and the peripheral autonomic nervous system, among others (Lotharius and Brundin, 2002; Taylor et al., 2009).

Alongside the cardinal motor phenotype, there are non-motor symptoms that can appear years earlier and may be unnoticed or

misinterpreted for prolonged periods. These symptoms constitute the prodromal phase of PD, an important period that leads to early diagnosis, and typically includes hyposmia, GI dysfunction, anxiety, depressive and apathetic-like behaviour, and dysautonomia. Furthermore, nocturnal sleep disturbances are also common, affecting 60-98% of patients, and include night-time awakenings, sleep fragmentation, and REM sleep disorder. Some of these symptoms do not respond to dopaminergic therapies and profoundly impair the patients' quality of life (Pfeiffer, 2003; Comella, 2007; Ziemssen and Reichmann, 2007). Still concerning the non-motor symptoms of PD, cognitive decline is detected at more advanced stages of the disease in a significant proportion of patients.

1.2.2. GENETIC BACKGROUND

Approximately 5-10% of PD patients have monogenic forms of the disease, with either an autosomal dominant or autosomal recessive pattern of inheritance (Saito et al., 2000). The identification of genetic defects linked to PD is growing and at least 13 loci and 9 genes were confirmed to be related, among them: α-synuclein (SNCA), parkin (PRKN), probable cation-transporting ATPase 13A2 (ATP13A2), leucine-rich repeat kinase 2 (LRRK2), PTEN-induced putative kinase 1 (PINK 1) and parkinson disease protein 7 or DJ-1, implying at least some genetic contribution in PD pathogenesis (Klein and Westenberger, 2012). These single gene defects are accountable for only a small number of PD cases, with the exception of LRRK2 gene which is the most representative cause of autosomal-dominant and sporadic forms of PD (Gilks et al., 2005). Until recently, there was only a small number of research reports looking into mitochondrial genetics and function in PD. Latest findings in PD brains and other tissues revealed abnormalities in complex 1 of the oxidative phosphorylation enzyme pathway, leading to cell dysfunction and death (Schapira, 2008). In addition, the investigations on single gene defects that are related to UPS, such as PRKN (an E3 ubiquitin ligase), have some potential to clarify the connection between PD and mitochondrial dysfunction. Furthermore, UPS failure leads to abnormal protein aggregation, including insoluble α-synuclein structures, which are the primary component

of Lewy bodies (LB) and Lewy neurites (Warner and Schapira, 2003; Betarbet et al., 2005), both histological hallmarks of PD.

1.2.3. HISTOLOGICAL MARKERS: LEWY BODIES

LB are intracytoplasmic spherical inclusions composed of insoluble aggregates of α-synuclein, ubiquitin, amyloid precursor protein and amyloid-beta peptides (Aβ), and represent the key feature for *post-mortem* assessment of PD. These structures are found in certain sites of neuronal loss, particularly the SNpc, but also the PFC, motor nucleus of the vagus nerve, hypothalamus, nucleus basalis of Meynert, LC and olfactory bulb (Forno, 1996). α-synuclein is a highly conserved presynaptic 140-amino acid phosphoprotein with chaperone-like structure. When present in high concentrations, monomeric α-synuclein can polymerize into filaments and fibrils, which can then form LB (Goedert, 2001). The presence of ubiquitin and other proteasomal subunits in LB suggests the involvement of α-synuclein and dysfunctional proteasomal degradation pathway in PD pathogenesis. Moreover, α-synuclein has been found to loosely bind and permeabilize monoaminergic vesicles, likely causing leakage of monoamines into the cytosol. In fact, Guo and colleagues identified a VMAT2-α-synuclein complex in which α-synuclein appears to down-regulate the activity of VMAT2 in vitro, increasing cytosolic DA and ROS (Guo et al., 2007).

1.2.4. TERAPHY

L-DOPA therapy started its revolution in the treatment of PD decades ago, and now DA replacement therapies in form of L-DOPA or DA agonist drugs are the standard therapeutics for PD patients. Even though it provides clear symptomatic relief to treated PD patients, improving daily living, employability and life span, it does not stop the progression of the disease. Despite of its effectiveness and suggestions of its protective and trophic effects, dopaminergic agents produce a scope of acute side effects resulting from activation of dopaminergic areas both in central and peripheral nervous

systems, including nausea, vomiting and hypotension. It is well admitted that the dopaminergic denervation of the basal ganglia in PD is uneven and these side effects are due to overstimulation in the ventral striatum where dopaminergic innervation remains fairly intact (Voon and Fox, 2007). Another challenging point verse on when L-DOPA treatment should be initiated, in view of high prevalence of poorly understood motor complications such peak-dose, biphasic dyskinesia, paradoxical involuntary movements, and unpredictable motor fluctuations. Moreover, dopaminergic drugs decline their effect and efficacy as the disease progresses, comprising events such "wearing off" (the same dose of L-DOPA lasts for a shorter period of time with a decrease of the antiparkinsonian effect before the next dose) and "freezing" (sudden shifts between mobility and immobility) (Stocchi et al., 2008).

Current pharmacologic interventions on motor symptoms of PD have also revealed the troublesome of treating simultaneously the diverse non-motor components, which may occur before (eg, constipation), during (eg, excessive sweating), or after (eg, dementia) the onset of motor deficits. Non-motor symptoms are only partially L-DOPA-responsive, and they remain largely refractory to existing interventions. The widespread neuronal loss that occurs in PD involving neurotransmitters other than DA may be the reason of the non-motor symptoms' unclear pathophysiology (Chaudhuri et al., 2006).

Such issues motivated the quest for other therapeutic approaches: studies on the neurorestorative effect of glial cell line-derived neurotrophic factor delivered into the nigrostriatal pathway, for instance, with promising signs of motor recovery in animal models of PD and PD patients (Saavedra et al., 2008); or technological interventions like electrical deep brain stimulation (DBS), considered the gold-standard therapy for PD nowadays. This technology relies on the implantation of chronic electrodes that modulate selected, focal basal ganglia structures, including the subthalamic nucleus and the globus pallidus, and it is advocated to patients developing the aforementioned motor complications to increasing amounts of medications required owing to progression of disease and worsening PD symptoms. The input of continuous electrical stimulation using brief >100 *Hz* pulses alleviates the same symptoms of PD that are relieved by L-DOPA therapy and

also reduces non-L-DOPA-responsive tremors with beneficial outcomes that exceed those achievable in comparable patients treated only with oral medication (Larson, 2014; Little and Brown, 2014).

1.3. ANIMAL MODELS OF PD

Mice, rats and nonhuman primates are the most broadly used animal models in PD studies. Briefly, injury or insults to DA-mediated pathways are replicated using a myriad of endogenous/exogenous toxins or genetic manipulations on these models. The ideal animal model exhibits a disease course of a few months or years during adulthood, with neuronal losses in the different dopaminergic brain areas exceeding 50%, clear motor disability that mimics PD, presence of LB, and, in case of a genetic manipulated models, a robust propagation of the mutation (Beal, 2001).

The major toxin-induced models are achieved by administration of neurotoxin 6-hydroxydopamine (6-OHDA) or systemic administration of the neurotoxin 1-methyl-4-phenyl-1,2,3,6-tetrahydropyridine (MPTP). Other less recurrent neurotoxin models involve administration of rotenone, paraquat, isoquinoline derivatives, or methamphetamine. Thus far, the dominance of motor-based animal models responsive to L-DOPA is solid. Although these models offer insight to possible causes of motor impairment, they fail to approach PD as a syndrome with complex extradopaminergic involvement and numerous non-motor features, and sometimes lack important hallmarks like the progressive nature of the pathology or LB occurrence (Langston, 2006).

The monogenic mutations seen in patients with familiar PD can be replicated in transgenic animal models, such as transgenic mice overexpressing normal or mutated human α-synuclein (Blesa et al., 2012). There are also models that attempt to genetically recreate the combination of destructive processes found in PD such as mitochondrial dysfunction, dysregulation of Ca^{2+} homeostasis, loss of trophic support or reduction of vesicular DA pool, which can be seen in mice with a drastic reduction of VMAT2 protein expression.

1.3.1. VMAT2 LO MICE

Several transgenic mouse lines with VMAT2 gene dysregulation have been generated. The complete deletion of the VMAT2 gene resulted in a weak animal with a lifespan of a few days after birth. This lethality provided evidence for the consequence of brutally reduced monoamine concentrations vital for monoaminergic signaling, as it has been seen in the past for TH knockout mice (Zhou et al., 1995). However, the mice that were heterozygous for VMAT2 displayed a 50% reduction in VMAT2 expression and were physiologically similar to the wild-type littermates, yet with a depressive-like phenotype. They did not display any motor signs of PD-like behaviour but manifested more marked deficits compared to wild-type animals when exposed with exogenous toxicants such as methamphetamine or MPTP (Takahashi et al., 1997). These susceptibilities showed that manipulating VMAT2 produced an increased sensitivity to PD-inducing toxins and demanded for a more profound disruption of the monoamine storage (Taylor et al., 2011).

A line of mice expressing only 5% of the VMAT2 protein (VMAT2-deficient, VMAT2 LO) was generated by Mooslehner and colleagues from the original colony at the Babraham Institute (Mooslehner et al., 2001). Briefly, the mouse VMAT2 locus was cloned from the 129/Sv genomic library and a 2.2 *kb* *Pvu*II fragment from the third intron of the VMAT2 gene, and then cloned into the blunt-ended *Not*I site of this construct. The targeting vector was introduced into 129/Ola CGR 8.8 embryonic stem cells and injected into blastocytes of C57BL/6 mice. Highly chimeric males were bred with C57BL/6 females. Originally, the C57BL/6 inbred strain of mice contained a spontaneous chromosomal deletion spanning the α-synuclein gene locus, although all traces of that mutation got eliminated later by Caudle and colleagues (Caudle et al., 2007).

VMAT2 LO mice are fully viable into adulthood and allow the study of reduced vesicular storage and poor monoaminergic innervation over an average lifespan of two years, among other PD-like features (Figure 1.4). They show severe reductions in DA, NE and 5-HT levels, increased oxidative stress, age-dependent loss of DA terminals and neurons in the SNpc/ VTA and

striatum with concomitant reduction in the metabolites DOPAC and HVA, and altered striatal neurotransmission and signaling, among others. Behaviourally, the VMAT2 LO exhibits several motor symptoms of PD which become progressively more severe with age, including reduced locomotor activity and impaired motor coordination (Taylor et al., 2011).

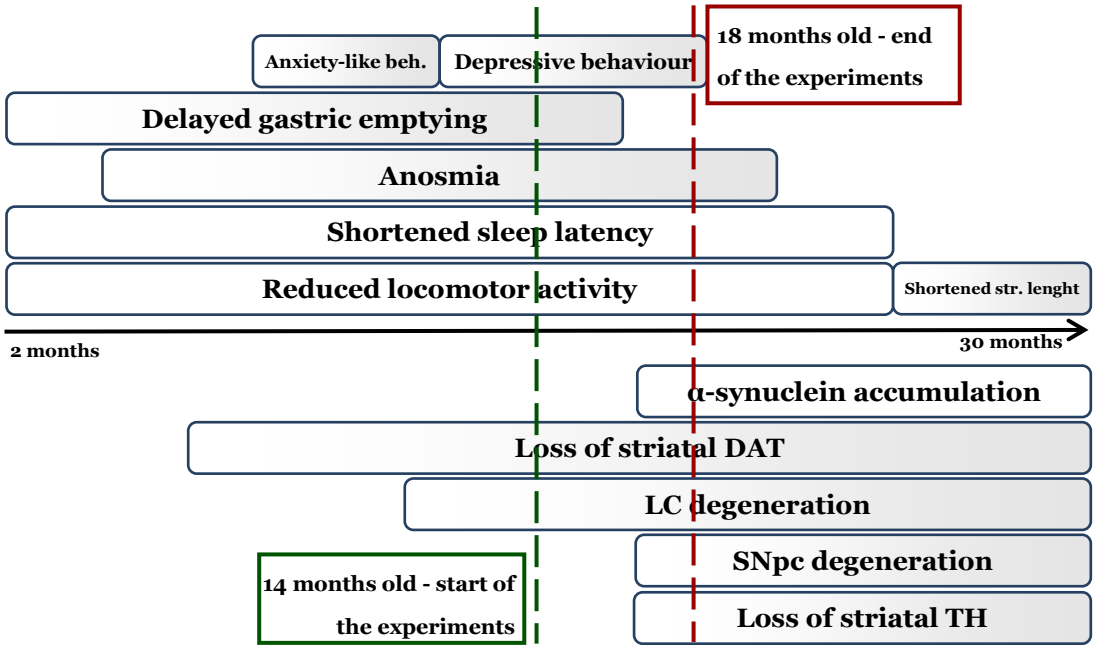

Figure 1.4 – Timeline of parkinsonian features observed in the VMAT2 LO mice mode from 2–30 months of age. Symptoms or pathology indicated by gradient colored box increased in severity as the mice aged. All boxes end at the last age the symptom or pathology was measured. (DAT: DA transporter; LC: locus coeruleus; SNpc: substantia nigra pars compacta; TH: tyrosine hydroxylase). Modified from Taylor and colleagues (Taylor et al., 2011).

The study of VMAT2 LO mice revealed that a general disturbance of monoamine storage and handling is one of the keys to almost fully reproduce the symptoms associated with the disease. Hence, using this new model in new adjunct therapeutic strategies for PD can offer important complementary information about new approaches within DA replacement therapy.

1.4. COMT INHIBITION

L-DOPA treatment is the broadest therapy for PD. The optimal dosing schedule for each patient is crucial to reduce the expected motor

complications. Changes in central pharmacokinetics underlie the development of L-DOPA-related motor fluctuations and dyskinesias, and the emergence of a L-DOPA 'threshold' for a response to the treatment. Increased doses of L-DOPA or smaller doses but administered more frequently may reduce these complications in the short-term but are not a durable solution (Stocchi et al., 2008).

Only 5-10% of the oral dose of L-DOPA/benserazide administered to patients crosses the blood-brain barrier (BBB). The inhibition of the decarboxylation pathway by benserazide shifts the metabolism of L-DOPA to COMT metabolic pathway. Taken together, the inhibition of CNS COMT in combination with L-DOPA/benserazide therapy can be the answer to more continuous availability of L-DOPA in the CNS after each dose. Tolcapone (Tasmar®) and entacapone (Comtess®/Comtan®) are the two selective reversible inhibitors approved for PD treatment, however entacapone only acts peripherally, consistent with literature indicating a marked COMT inhibition by Tolcapone (Deane et al., 2004) (Figure 1.5).

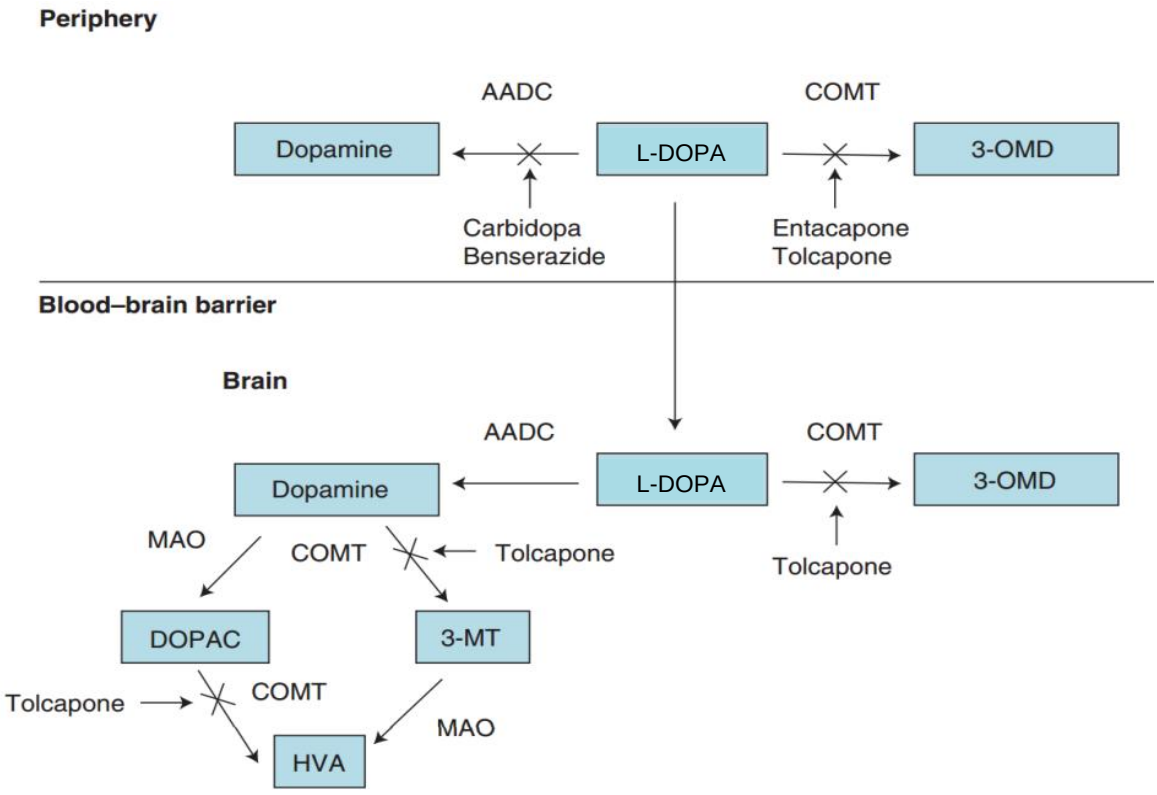

Figure 1.5 – Central and peripheral effects of COMT inhibition in L-DOPA metabolism. (3-OMD: 3-O-methyldopa; AADC: Amino acid decarboxylase; COMT: Catechol-O-methyltransferase; DOPAC: 3,4-Dioxyphenylacetic acid; HVA:

Homovanillic acid). Modified from Leegwater-Kim and Waters (Leegwater-Kim and Waters, 2006).

Tolcapone (3,4-dihydroxy-4′-methyl-5-nitrobenzophenone) is a second-generation, highly selective, orally-active COMT inhibitor. It increases the plasma levels of L-DOPA 1.3 to 2.1-fold and prolongs its duration of action 1.1 to 1.8-fold by reducing its metabolism to 3-OMD.

The addition of the COMT inhibitor Tolcapone in fluctuating PD patients under L-DOPA regime showed indeed an improvement of motor scores and decrease in average L-DOPA daily dose. However, rare hepatotoxicity situations in Tolcapone-treated patients raised some concern after liver function tests showed abnormalities, especially among patients with moderate cirrhotic liver disease. Tolcapone has been associated with increased levels of serum glutamic pyruvic transaminase/alanine aminotransferase (ALT) and serum glutamic-oxaloacetic transaminase/aspartate aminotransferase (AST), whereby it should be used with caution and requires liver function monitoring. The mechanism underlying possible Tolcapone-induced liver damage may relate to abnormalities in mitochondrial respiration in hepatocytes due to uncoupling of oxidative phosphorylation (Borges, 2005). Other side-effects include new or worse dyskinesias, nausea and diarrhea, and sleep disturbances (Leegwater-Kim and Waters, 2006).

The increase of 3-OMD by metabolism of L-DOPA via COMT is associated with conversion of SAM to SAH, and SAH is subsequently cleaved to homocysteine (Hcy) (Figure 1.6). In fact, hyperhomocysteinemia (HHcy) is seen in L-DOPA treated PD patients. Elevation in total Hcy (tHcy) is a suggested risk factor for stroke, coronary artery disease, and dementia beside others.

In order to achieve a tHcy reduction, supplementation of vitamin B6 (trans-sulfuration pathway) or vitamin B12 and folic acid (re-methylation pathway) are suggested on one hand and inhibition of COMT on a regular basis on the other. Since Tolcapone can cross the BBB, central COMT inhibition may hypothetically be neuroprotective in the long term, by reducing enduring degenerative changes and dementia associated with HHcy. Nevertheless, when COMT extensive detoxification role within the brain is

repressed, DA metabolism is forced to go further down to neurotoxic N-methyl-4-phenylpyridine-like substrates, which brings unforeseen consequences (Müller and Kuhn, 2006).

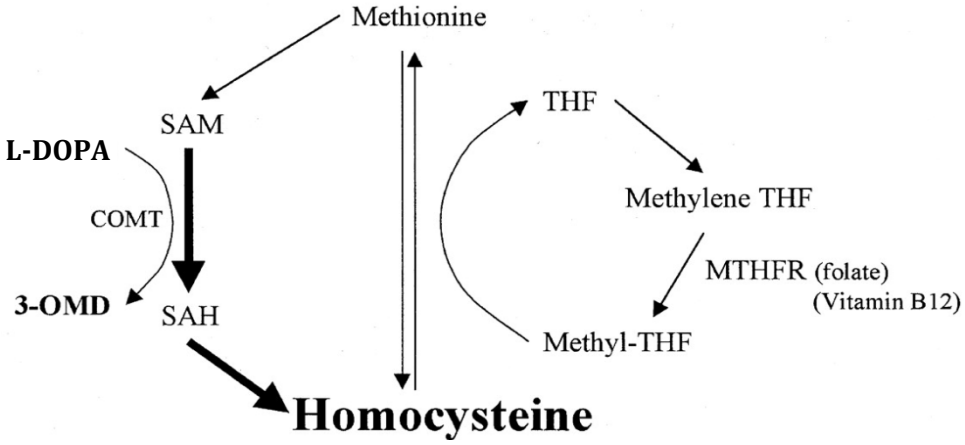

Figure 1.6 – Metabolism of L-DOPA to 3-OMD causes an increase in the formation of SAH, which is immediately metabolized to Hcy. (3-OMD: 3-O-methyldopa; COMT: catechol-O-methyltransferase; Methylene THF: methylene tetrahydrofolate; MTHFR: methylenetetrahydrofolate reductase; SAH: S-adenosylhomocysteine; SAM: S-adenosylmethionine). Modified from Postuma and Lang (Postuma and Lang, 2004).

1.5. AIM OF THE STUDY: INHIBITING COMT IN VMAT2 LO MICE UNDER L-DOPA TREATMENT

Altogether, we hypothesized Tolcapone to be effective as vascular and neuronal protector in PD, therefore improving functional outcome. Thus, as a novel concept, the aim of this study is to investigate the effect of COMT inhibition over behavioural, biochemical and histological outcomes in the context of PD in VMAT2 LO mice during the '*off*' period of L-DOPA treatment. To achieve this, pharmacological inhibition of COMT with Tolcapone was performed in a VMAT2 LO and wild-type mice under L-DOPA/benserazide treatment. Baseline and post-treatment changes in motor, olfactory and cognitive function were tested, as well as food intake, during periods without any treatment. Additionally, liver integrity was assessed by measuring the levels of ALT and AST. It is intended to also quantify tHcy levels in peripheral blood (to evaluate vascular protection) and immunohistochemical signs of neurodegeneration (to evaluate neuronal protection) at a later time point.

CHAPTER 2

Materials and Methods

2.1. STUDY DESIGN

All experimental procedures were performed under the license n. ZH 205/2012 and approved by both local and federal Swiss authorities. This study design was based on the availability of VMAT2 LO animals within the colony of the Animal Sleep Laboratory of the University Hospital of Zurich (USZ), and ran throughout February 2015 to mid-September 2015.

The 119-day chronic experimental period began with one week of baseline behavioural testing and tail blood sampling followed by four more rounds of tests and blood collection ('*off*' period), spaced by three weeks of pharmacological treatment ('*on*' period). Oral administrations took place twice a day (8.00*h* or 9.00*h*, according to season, and 8 hours later). After the last round of tests, mice were euthanized, and brains and livers collected for posterior evaluations.

In order to work with robust results, the behavioural data presented in this thesis only comprise the period between baseline and the end of the 2nd round, the so called sub-chronic window. This choice was made due to the low number of experimental subjects in the VMAT2 LO groups between 3rd and 4th rounds, which are still running. However, the food intake test and quantification of plasma AST and ALT were performed during and after the 4th round, respectively (Figure 2.1).

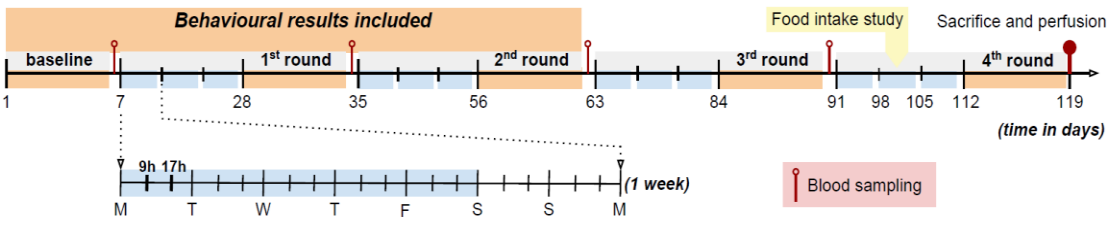

Figure 2.1 – Chronologic representation of the experimental period, accounting all the treatment and behavioural testing weeks. The subjects

were not treated during weekends and during behavioural testing week, to avoid an acute effect of the pharmacologic interventions.

2.1.1. EXPERIMENTAL ANIMALS

Male, adult C57BL/6J mice were used in all the experiments. VMAT2 LO mice on a C57Bl/6 background were originally obtained from Jackson Laboratories and then bred in-house (BZL, USZ). Wild-type control C57BL/6 mice were obtained from the group's colony or ordered (Janvier Labs, Le Genest-Saint-Isle, France). Male mice were used to avoid the influence of hormonal cycles on behaviour. Until the presentation of this thesis, the study comprised 43 mice, 24 wild-type and 19 VMAT2 LO, aged 14 months ± 18 days on the first day of baseline behavioural testing.

All animals were single housed in clear-transparent Euro-standard Type II L plastic cages (530 cm^2 floor area, Indulab AG, Gams, Switzerland), containing autoclaved dust-free sawdust bedding, one cardboard mouse house (12 *cm* x 12 *cm* x 6 *cm*) and one facial tissue (20 *cm* x 20 *cm*) as nesting material. Tap water and regular chow (Provimi Kliba SA, Kaiseraugst, Switzerland) were provided ad libitum throughout the experiments. Both the stock and the experimental room were maintained on a 12 *h* light/dark cycle (lights on at 8.00*h* or 9.00*h*, according to season), and constant temperature (21 - 23 °*C*) and relative humidity (30%). All mice were weighed daily until completion of the studies. The animals had a period of acclimation to the room before all experimental procedures.

2.1.1.1. GENOTYPING AND PCR ANALYSIS

All VMAT2 LO subjects were obtained from the group's colony. These animals were permanently identified with ear punch numbering system, which can provide enough tissue for PCR screening. PCR analyses were made throughout the study using a PCR kit (DNeasy® Blood & Tissue Kit, Qiagen, Germany) to determine the genotype of the experimental animals. Genotypes were further confirmed from DNA extracted from tail samples taken immediately prior to the sacrifice of the animals.

Briefly, the PCR protocol was performed with the forward primer F330KA1 (5'-GCGAATATTCCAGTCCTCCA-3') and the reverse primer KAR (5'- CAGGCAACACCAGAAACAAT-3') for VMAT2 WT and RKA835 (5'-GGAAAGTGAGCCACCATGTAG-3') for VMAT2 LO. Amplification was performed in a 25 μL reaction mixture with 9.5 μL nuclease free water, 1 μL forward primer (10 μM), 0.5 μL of each reverse primer (10 μM), 12.5 μL GoTaq green master mix (Promega, Madison, Wisconsin, USA) and 1 μL of DNA using a standard thermocycler (TProfessional; Biometra, Göttingen, Germany). PCR cycle started with 4 minutes of initial denaturation at 94°C, followed by 25 repeated cycles of 1 minute denaturation at 94°C, 1.5 minutes annealing at 57 °C and 1 minute of extension at 72 °C, and ended with 7 minutes of final extension at 72 °C. PCR products were stained with GelRed (Biotium, Hayard, California, USA) separated with electrophoresis at 150 V for 1 hour in a 3% agarose gel (w/v) in 1x TAE buffer and visualized under UV light (Figure 2.2).

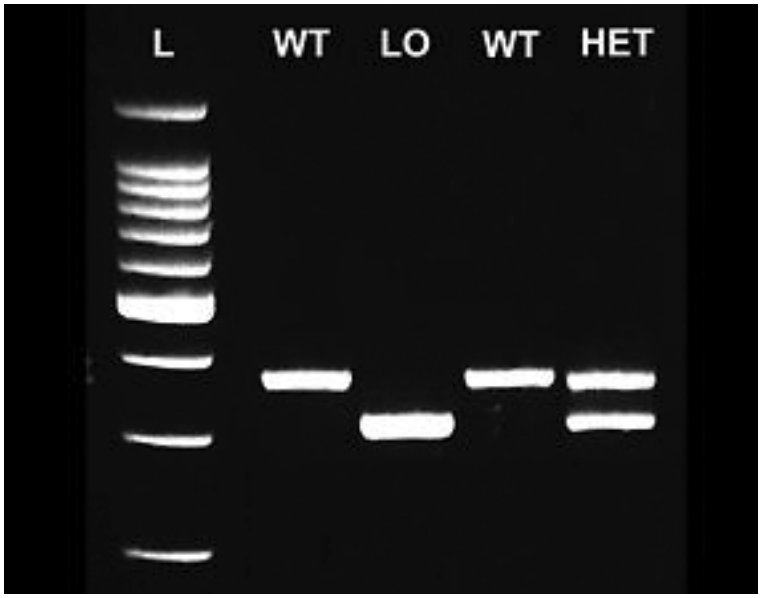

Figure 2.2 – Confirmation of the PCR products by gel electrophoresis. The 3% agarose gel is visualized under UV light and the resultant bands are identified as VMAT2 wild-type, VMAT2 LO and VMAT2 heterozygous.

2.1.2. PHARMACOLOGIC TREATMENTS

Mice were grouped into four treatment groups per genotype and distributed according to body weight and baseline tests' performance, in order to certify balanced groups. The different treatments consisted of: saline

solution (NaCl 0.9% in water, 1 $\mu L.kg^{-1}$, *pH* 7, Grosse Apotheke Dr. G., Bichsel AG, Switzerland) as placebo; 20 $mg.kg^{-1}$ L-DOPA/benserazide (Madopar® 125 *mg*, *pH* 6.1, Roche Pharma AG, Switzerland), 15 $mg.kg^{-1}$ Tolcapone (Tasmar® 100 *mg*, *pH* 5.7, MEDA Pharma GmHB, Switzerland); and an equitable solution of 12.5 $mg.kg^{-1}$ L-DOPA/benserazide and 15 $mg.kg^{-1}$ Tolcapone (Table 2.1). The concentration of drug in the L-DOPA/benserazide group represents the ordinary dosage (12.5 $mg.kg^{-1}$) increased 1.6-fold, in order to mimic the bioavailability of DA on the groups treated with L-DOPA/benserazide + Tolcapone.

Table 2.1 – Overview of the experimental groups. Groups' distribution per genotype, doses administered in each one, and the number of animals in experiment and with the treatment complete until the final of the 2nd round of experiments.

GROUP	GENOTYPE	LEVODOPA MADOPAR®	TOLCAPONE TASMAR®	TOTAL NUMBER OF ANIMALS IN EXPERIMENT	NUMBER OF ANIMALS WITH TREATMENT COMPLETE UNTIL THE SECOND ROUND
1	VMAT2 WT	NaCl		6	6
2		20 $mg.kg^{-1}$	-	6	6
3		-	15 $mg.kg^{-1}$	6	6
4		12.5 $mg.kg^{-1}$	15 $mg.kg^{-1}$	6	6
5	VMAT2 LO	NaCl		6	5
6		20 $mg.kg^{-1}$	-	5	4
7		-	15 $mg.kg^{-1}$	5	5
8		12.5 $mg.kg^{-1}$	15 $mg.kg^{-1}$	6	5

Drug suspensions were prepared no more than 3 days before each treatment week, aliquoted at -80 ^{o}C and administered at 0.5 – 1 $mL.kg^{-1}$. During administration, drug vials were vigorously mixed to certify the homogeneity of the suspensions. All mice received 120 doses of the corresponding treatment throughout the 119 days experimental period. The doses were orally administered using a pipette 10 – 100 μL, and reported at the quality control as *Good* or *Irregular*. All mice under 50 *g* of body weight

received daily wet-food (50-75% water) *ad libitum* in addition to the regular chow.

2.1.3. BEHAVIOURAL TESTS

All tests were performed during the light cycle, with room illuminance by white fluorescent lightbulbs of 90 *lux*. Prior and in between all training and testing trials, the behavioural apparatuses were cleaned with a mild, non-toxic water-based detergent (10% ethanol + 0.5% TEGOL).

There were three behavioural tests to assess motor outcomes: open field test, rotarod test and bar test; and two to evaluate non-motor behaviour: olfactory discrimination test and novel object recognition test. All tests were conducted on three or four consecutive days, following the same order and at the same time of day.

2.1.3.1. OPEN FIELD TEST

The open field test (Bello et al., 2011) is a common measure of exploratory behaviour in mice. This test was assayed to evaluate the spontaneous locomotor activity, namely the distance travelled, of VMAT2 WT and VMAT2 LO mice.

The apparatus assembles 4 identical plexiglas boxes (46 *cm* x 46 *cm* x 40 *cm*) and a video camera connected to an automated tracking system (EthoVision XT 9.0, Noldus, Germany) (Figure 2.3). Animals were habituated to the setup for 15 minutes on the day before the baseline testing. The actual test on the following day served as habituation for the non-motor tests on the subsequent days. Each trial had up to 4 animals simultaneously which were allowed to explore the arenas freely for 30 minutes. In this test, the total distance traveled (in centimeters) was the output parameter, which was plotted by treatment group and over time.

Figure 2.3 – Top view of the open field apparatus. Four plexiglas adjacent boxes are separated with wood dividers to avoid animals' eye contact, and placed over an infrared light. A ceiling hanging infrared camera captures the movements of the multiple subjects and sends the data to a PC for storage and analysis.

2.1.3.2. ROTAROD TEST

To assess the motor coordination in VMAT2 WT and VMAT2 LO mice, a rotarod test was carried out (Avale et al., 2003).

A standard mouse rotarod machine with a horizontally oriented, rotating cylinder, integrated timers and falling sensitive platforms (UgoBasile©) was set to constant 16 revolutions per minute and could accommodate 5 mice simultaneously (Figure 2.4). A 10-minutes training session was assayed 3 hours before the test. During this training, mice were repeatedly repositioned on the rod after each fall, in order to maximize the learning period. During the testing phase, the animals were placed onto the rotating treadmill until a maximum time of 180 seconds. A second chance was given for those who fell meanwhile. The higher latency to fall (in seconds) extracted from both attempts was considered for the analysis, and plotted by treatment group and round of experiments.

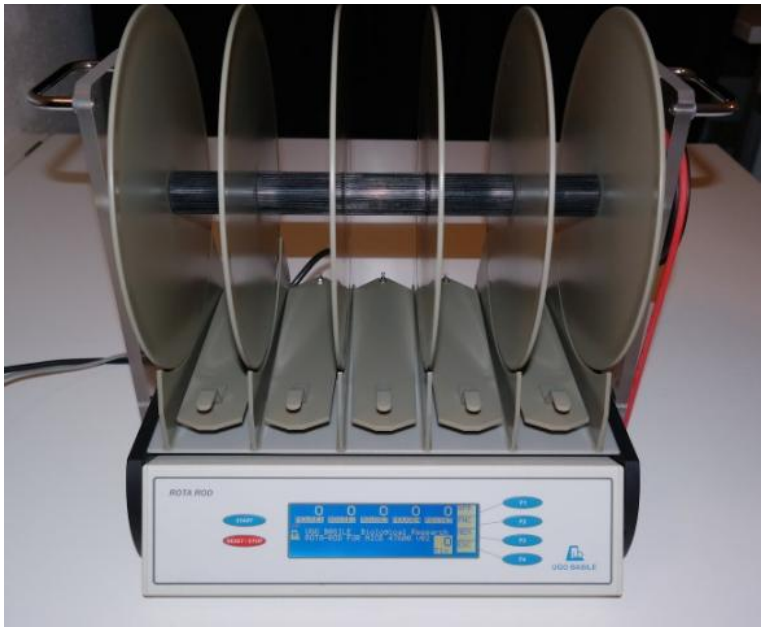

Figure 2.4 – Front view of the rotarod machine (UgoBasile©). The equipment has a horizontally oriented, rotating cylinder 15 *cm* high, integrated timers and falling sensitive platforms that can accommodate 5 mice simultaneously, facing a wide black curtain.

2.1.3.3. BAR TEST

The bar test (Noain et al., 2013) was conducted to examine the body rigidity or catalepsy related to impaired dopaminergic neurotransmission in the nigrostriatal pathway.

The animals were placed sitting on the working table over their hind paws and grabbing a 4 *cm* elevated acrylic bar (1 *cm* diameter) with their front paws (Figure 2.5). Immediately after, the timer was started. A trial was considered valid when the animal remained grabbing the bar with the front paws at least 1-2 seconds (until the timer was running). Usually, 1-3 trials were invalid for each mouse at the beginning of the testing session. The time of immobility was counted in 5 trials with a 180 seconds cutoff for each trial. For the analysis, a trimmed mean was calculated discarding the lowest and the highest time values for each mouse over the 5 trials and the results were plotted by treatment group and round of experiments.

Figure 2.5 – Bar test apparatus. The 4 *cm* elevated acrylic bar and both plastic bases were fixed to the surface with white tape. The test is done facing a wide black curtain.

2.1.3.4. OLFACTORY DISCRIMINATION TEST

The olfactory discrimination test was applied in the study as a test control for non-responsiveness to L-DOPA/benserazide plus Tolcapone therapy, as it is known that DA replacement therapy has no effect over this phenotype (Taylor et al., 2011).

The experiments were adapted from Taylor and colleagues (Taylor et al., 2009). Two 100% cotton odorless discs (~6 *cm* diameter) were placed into labeled falcon tubes containing bedding from each test animal's cage for at least 12 hours. During the test, the mouse was presented with one cotton disc scented with its own bedding and a cotton disc scented with another mouse's bedding (Figure 2.6). Along all the rounds of experiments, the positions of the discs were alternated, to avoid place preferences. Sniffing was defined when the animal's nose was located within a zone 2 *cm* or less from each disc. The cumulative time spent within both these zones was recorded during a 2-minutes trial starting from the moment the nose point was detected inside any of the aforesaid zones. For the analysis, the recognition index was calculated as the cumulative time spent sniffing the disc scented with a foreign animal's bedding divided by the total cumulative time spent sniffing both discs and presented by treatment group and round of experiments.

Figure 2.6 – View of the open field with cotton discs for the olfactory discrimination test. The discs were fixed to the base always in the same side of the arena and the mouse is placed on the other side, in the middle, facing the discs.

2.1.3.5. NOVEL OBJECT RECOGNITION TEST

The novel object recognition test was performed in the interest of evaluate the effect of Tolcapone treatments on episodic memory (Büchele et al, 2015).

The novel object recognition test consisted of a training phase followed by a testing phase 3 hours later. During the training phase, two identical small objects were placed in both corners of one side of the open field. Mice were placed in the opposite side facing the objects (Figure 2.7) and left free to explore during 5 minutes. During the testing phase, one object was replaced by a novel one, different in colour, shape and texture. The animals were placed again in the opposite side facing the objects and left to explore for 3 minutes. Here, the position of the new object was also alternated with the familiar counterpart over all the rounds of experiments, to avoid side preferences. An approach was considered valid every time the nose-point could be detected inside an area of 2 *cm* from the limits of that same object. The cumulative time spent exploring each object was recorded. Since the novelty factor is crucial in this test, the objects were not repeated for the same animal throughout all the experiments. However, the objects were saturated

with smelling cues due to reuses over the years, which required a vigorous cleanliness with 70% ethanol solution before and after every training and testing trial. Moreover, the animals that did not show any exploratory interest for any of the objects during the testing phase, performed again on the same day, with a new set of objects. For the analysis, the recognition index was calculated as the cumulative time spent inside the novel object zone divided by the total cumulative time spent inside both zones and plotted by treatment group and round of experiments.

Figure 2.7 – View of the open field with two different objects for a novel object recognition trial. The objects were fixed to the base of the arena and the mouse is placed on the other side, in the middle, facing the objects.

2.1.4. FOOD INTAKE

VMAT2 LO mice show a clear distinct body complexion compared to wild-type mice since birth. They require a period of up to 1 month with the progenitors until weaning (instead of the standard 21 days), a special feeding-program afterwards and their littermates company. Visually, they are smaller and less vigorous, but the relation of these features with the feeding behaviour is unclear. Since there is no information about this aspect, the chance of characterizing food intake in VMAT2 LO mice was taken, together with the analysis of the different treatments' influence on the subjects' feeding behaviour.

Between the 99th and the 103rd day of treatment, all the dry food was removed from the cages and every mouse was presented only with a cup (w = 2.37±0.005 g) containing wet food (74±0.5% water). Each mouse received at 17.00h between 30-60 g of wet food (x_i), prepared 24 hours earlier. There were also prepared 8 labeled control cups, with 10-70 g portions, placed in empty cages in the stockroom, intended to determine the percentage of weight lost by overnight water evaporation E_1 (17.00h - 9.00h) and percentage of weight lost by water evaporation during day E_2 (9.00h - 17.00h) as a function of total weight of the cup. At 9.00h and at 17.00h, the test and control cups were weighed (x_{ii} and x_{iii}, respectively).

To calculate the food intake f_{total} in $g.24h^{-1}$, based on visual observations showing that mice start eating not long after the wet food is offered and excluding the water of the eaten portion, the following formula was applied:

$$f_{total} = 0.26 \cdot [(x_i - x_{ii}) - E_1(x_i) \cdot (x_{ii} - w)] + \alpha \cdot [(x_{ii} - x_{iii}) - E_2(x_{ii}) \cdot (x_{iii} - w)]$$

with $\alpha = 0.26 + 0.74 \cdot [E_1(x_i) + E_2(x_{ii})]$

The results were plotted by genotype.

2.1.5. BLOOD COLLECTION FOR DETERMINATION OF tHCY AND LIVER ENZYMES

In order to avoid stress-related outcomes, blood collections took place between 7-9 days after the last treatment day of each round, after the behavioural testing phase. No more than 10% of total circulating blood volume was collected, without anesthesia, from tail vein into lithium-heparin coated tubes (Microtainer®, BD, Switzerland). Some mice did not undergo blood sampling because they were too big for the restrainer (Figure 2.8). At the final timepoint, <600 μL of blood was taken directly from the right atrium immediately before the perfusion procedure.

The metabolites of interest were tHcy and the liver enzymes AST and ALT. tHcy levels were intended to be analyzed at baseline, between 2nd and 3rd rounds, and at final endpoint from blood samples of all subjects at the

research laboratory of the neurology department (USZ) using an absorbance kit (Mouse Homocysteine Kit, Crystal Chem, The Netherlands). The liver enzymes were examined in the samples from the final endpoint from the VMAT2 WT control and VMAT2 WT L-DOPA/benserazide + Tolcapone groups at the Institute for Clinical Chemistry (USZ).

Figure 2.8: Materials for blood sampling. The blood is collected with a 1 *mL* insulin syringe and transferred to a lithium-heparin coated tube.

2.1.6. PERFUSION AND TISSUE PRESERVATION

Mice were sacrificed by classic full-body transcardiac perfusion. Briefly, subjects were anesthetized with sodium pentobarbital (50 $mg.kg^{-1}$, i.p.). After fixation and chest opening, the liver was visually evaluated and photographed, the heart right atrium was incised and blood collected to a lithium heparin gel coated tube (Figure 2.9).

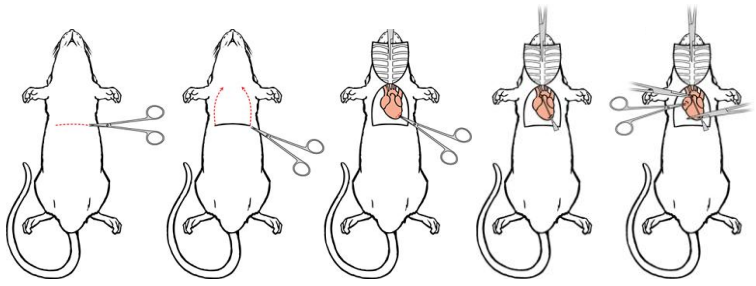

Figure 2.9: Schematic procedure of full-body transcardiac perfusion in mice. The anesthetized mouse is fixed to the working platform and the chest is open. The right atrium of the heart is perforated (with collection of the blood) and the

exsanguination was performed by intracardiac perfusion into the left ventricle of the heart. Modified from Gage and colleagues (Gage et al., 2012).

Complete exsanguination was performed by intracardiac perfusion of ice-cold phosphate–buffered saline (PBS) into the left ventricle of the hearth. The animal was fixed by subsequent perfusion of 4% paraformaldehyde (PFA) in PBS. Afterwards, the liver and the brain were immediately removed, post-fixed and cryoprotected by dehydration in a 4% PFA/ 15% sucrose in PBS solution, at 4 $℃$ for 12h, to avoid freezing effect during cryosectioning. A following step of dehydration in 30% sucrose in PBS occurred at 4 $℃$ for 24h. Finally, the organs were placed in cryomolds, frozen in 30% sucrose in PBS solution and stored at -20 $℃$ until further use.

2.2. STATISTICAL ANALYSIS

In all experiments, data are presented as means ± SEM. Repeated-measures ANOVA with nested factors followed by Bonferroni *post hoc* analysis, one-way ANOVA, unpaired Student's t-test two-tailed and one sample t-test were applied as appropriate using IBM SPSS Statistics 22.0.0.1 and GraphPad Prism 5.0.4 for Windows. A value of p<0,05 was considered statistically significant.

CHAPTER 3

Results

As previous mentioned, the results presented in this thesis are only concerning the baseline, 1st and 2nd rounds for the sake of group power. However, quantifications of food intake and blood markers of liver damage were assessed at the last round and are also shown here.

The rate of successfull doses administration throughout the study stands very high, with only 2.53% of them being *Irregular*.

3.1. AGE, BASELINE BODY WEIGHT AND BODY WEIGH PROGRESSION OF VMAT2 WT AND VMAT2 LO MICE

Mice around 14 months of age at baseline were included in this study (Figure 3.1*A*). They were distributed within the batches and the treatment groups in a way that minimized the age variability between groups. The mice were weighted every weekday throughout the experiments. In order to

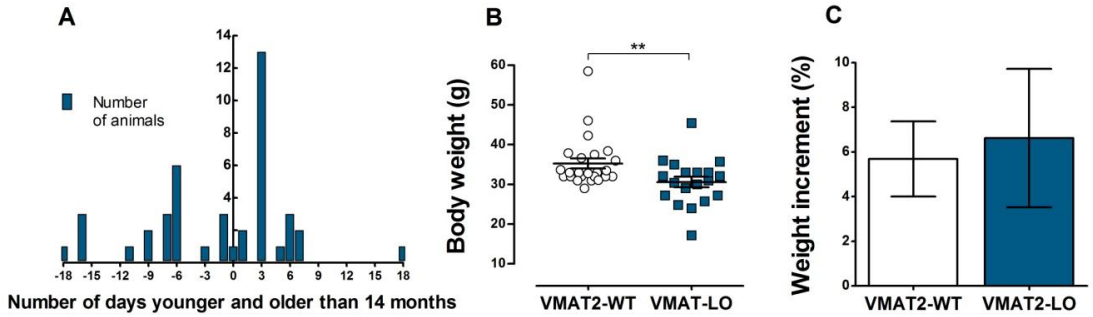

Figure 3.1: VMAT2 LO mice display a significantly low body weight at 14 months of age and similar weight increment. ***A***, distribution of all subjects' ages at the 1st day of experiments (n=43). ***B***, VMAT2 LO mice show a significantly reduced body weight at 14 months of age compared to VMAT2 WT. Results represent the mean of body weight of all subjects (g) ± SEM per genotype (VMAT2 WT=24, VMAT2 LO=19, $^{**}p<0{,}01$). ***C***, Weight increment on both genotypes at the end of 2nd round is similar (VMAT2 WT=24, VMAT2 LO=19). Results represent the mean increment in body weight (% of body weight at baseline) ± SEM per genotype.

characterize the VMAT2 LO mice concerning their body weight, all measures from baseline were confronted. The VMAT2 LO mice show a significant lower body weight compared to VMAT2 WT mice (unpaired *t*-test two-tailed, $^{**}p<0{,}01$; Figure 3.1*B*). The weight increment was also evaluated 56 days after baseline, i.e. until the end of the 2nd round. The weight increment analysis shows no significant differences between the treatment groups in either genotype (data not shown). Moreover, the weight increment of VMAT2 LO mice is similar to the VMAT2 WT controls (unpaired *t*-test two-tailed, $p>0{,}05$; Figure 3.1*C*).

3.2. FEEDING BEHAVIOUR

The food intake of the mutant line was evaluated between the 99th and the 103rd days of treatment. Since all subjects were on a wet-food diet (74±0.5% water), an established procedure was used so that the consumption of actual chow could be extracted from each measurement, minimizing the inaccuracy of the test. The data was merged into genotypes, as the treatments show no effect on the feeding behaviour of the animals (data not shown). Although the subjects of both genotypes consume the same amount of food per day (unpaired *t*-test two-tailed, $p>0{,}05$; Figure 3.2*A*), the results show a significant increase of the food intake in relation to body weight in VMAT2 LO compared to VMAT2 WT (unpaired *t*-test two-tailed, $^{*}p<0{,}05$; Figure 3.2*B*).

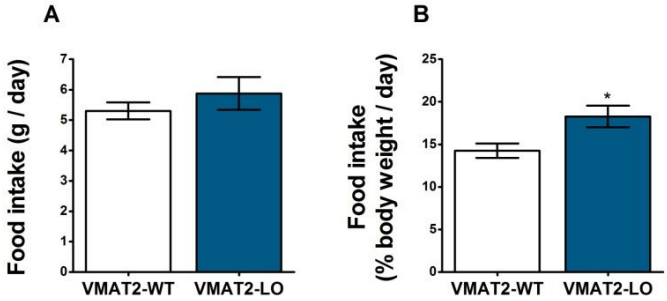

Figure 3.2: VMAT2 LO mice eat significantly more than VMAT2 WT mice in relation to their own body weight, despite of both genotypes have shown similar food consumption. ***A***, VMAT2 WT and VMAT2 LO mice show a similar result regarding the mean amount of eaten chow (*g*) ± SEM per genotype per day (VMAT2 WT=23, VMAT2 LO=9). ***B***, VMAT2 LO mice reveal an exacerbated food intake compared to VMAT2 WT subjects. Results represent the mean food intake (% of body weight) ± SEM per genotype per day (VMAT2 WT=23, VMAT2 LO=9, $^{*}p<0{,}05$).

3.3. BEHAVIOURAL TESTS

3.3.1. LOCOMOTOR ACTIVITY

The open field test (Bello et al., 2011) was performed to evaluate the effect of Tolcapone treatments on the spontaneous locomotor behaviour of VMAT2 WT and VMAT2 LO mice under L-DOPA treatment.

The results show a significant difference at baseline between VMAT2 WT and VMAT2 LO mice (unpaired *t*-test two-tailed, ***p<0,001; Figure 3.3*A*), with a marked hypolocomotion in the mutant group. However, no major differences are seen between the treatment groups within each genotype after the 1st and 2nd rounds of testing (repeated measures ANOVA with nested factors, p>0,05; Figure 3.3*B* and 3.3*C*, respectively).

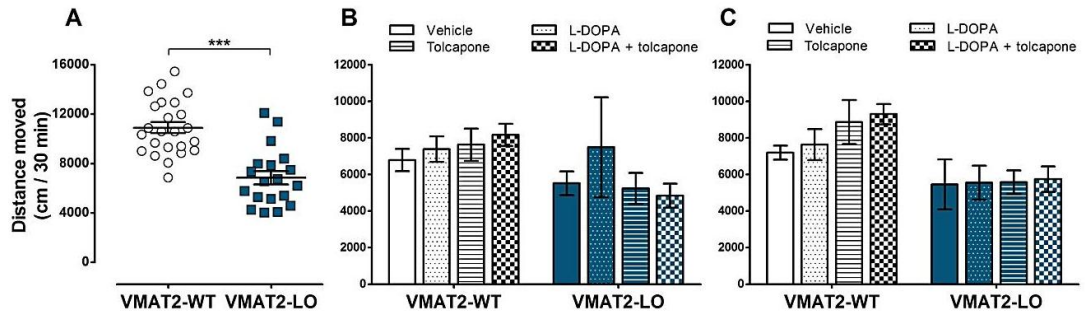

Figure 3.3: VMAT2 LO mice exhibit hypolocomotor activity at baseline and do not respond to pharmacological interventions. ***A***, VMAT2 LO mice show a substantial reduction in distance travelled at 14 months of age compared to WT controls. Results represent the mean distanced moved (cm / 30 min) ± SEM per genotype (VMAT2 WT=24, VMAT2 LO=19, ***p<0,001). The treatments did not show a significant effect in either genotype at 1st (***B***) and 2nd (***C***) rounds. Results represent the mean distanced moved (cm / 30 min) ± SEM per treatment group (VMAT2 WT: Vehicle=6, L-DOPA=6, Tolcapone=6, L-DOPA + Tolcapone=6; VMAT2 LO: Vehicle=5, L-DOPA=4, Tolcapone=5, L-DOPA + Tolcapone=5).

The results show a significant negative progression of exploratory behaviour in all VMAT2 WT groups due to habituation effect from baseline to 1st and 2nd rounds. The VMAT2 LO treated with saline is the only group of the mutant line that experiences this affect, while the remaining groups of VMAT2 LO show no contextual memory formation (repeated measures ANOVA with nested factors, *p<0,05; **p<0,01; ***p<0,001; Figure 3.4).

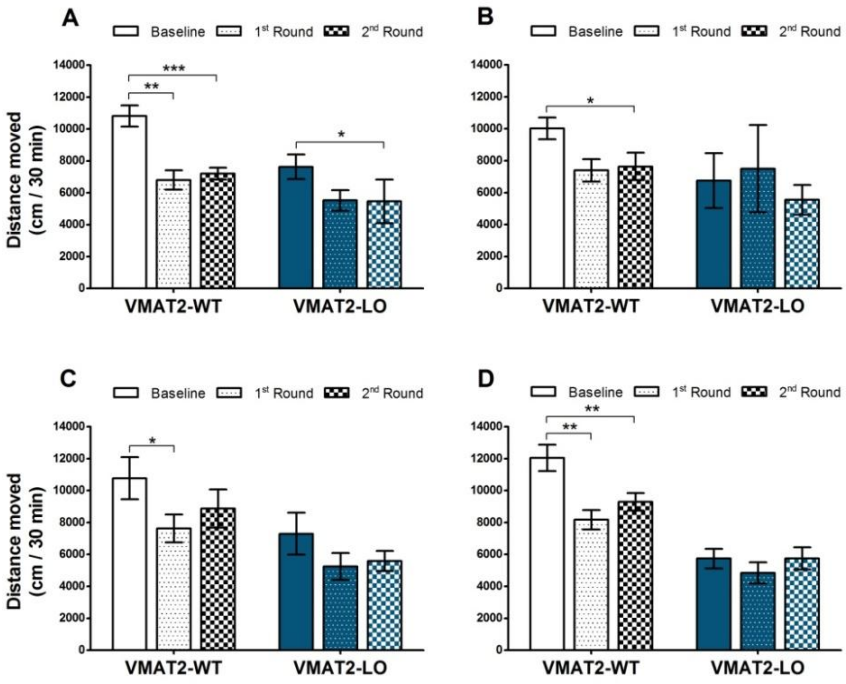

Figure 3.4: The habituation effect over time in VMAT2 LO and VMAT2 WT controls. VMAT2 WT mice of all treatment groups show a substantial reduction in distance travelled throughout the study while VMAT2 LO of the vehicle group are the only ones that appear to form a contextual memory. Results represent the mean distanced moved (cm / 30 min) ± SEM for ***A***, vehicle groups (VMAT2 WT=6, VMAT2 LO=5), ***B***, L-DOPA groups (VMAT2 WT=6, VMAT2 LO=4); ***C***, Tolcapone groups (VMAT2 WT=6, VMAT2 LO=5); ***D***, L-DOPA + Tolcapone groups (VMAT2 WT=6, VMAT2 LO=5); **p*<0,05; ***p*<0,01; ****p*<0,001.

3.3.2. MOTOR COORDINATION

To evaluate the effect of Tolcapone treatments over motor coordination in VMAT2 LO mice and their VMAT2 WT controls, a rotarod test (Avale et al., 2003) was carried out as described earlier.

At 14 months of age, the motor coordination of VMAT2 LO mice is considerably reduced as compared to their VMAT2 WT controls (unpaired *t*-test two-tailed, ****p*<0,001; Figure 3.5*A*). The treatments show the absence of a consolidated or significant effect on both genotypes at 1st and 2nd rounds of testing (repeated measures ANOVA with nested factors, *p*>0,05; Figure 3.5*B* and 3.5*C*, respectively).

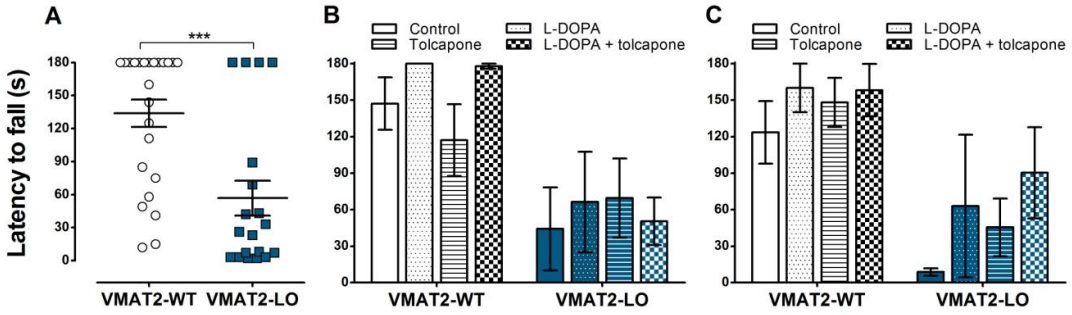

Figure 3.5: VMAT2 LO mice display weaker motor coordination at baseline and do not respond significantly to the interventions at 1st and 2nd rounds. ***A***, VMAT2 LO mice show a severe motor disturbance by low individual times onto the rotating rod at 14 months of age. Results represent the mean latency to fall (s) ± SEM per genotype (VMAT2 WT=24, VMAT2 LO=19, ***p<0,001). ***B*** and ***C***, The treatments did not show a significant change in any of the groups at 1st and 2nd round, respectively. Results represent the mean latency to fall (s) ± SEM per treatment group (VMAT2 WT: Vehicle=6, L-DOPA=6, Tolcapone=6, L-DOPA + Tolcapone=6; VMAT2 LO: Vehicle=5, L-DOPA=4, Tolcapone=5, L-DOPA + Tolcapone=5).

The time progression on each treatment and genotype shows no significant differences but some tendencies can be depicted, especially the worsening of VMAT2 LO mice treated with vehicle (repeated measures ANOVA with nested factors, p>0,05; Figure 3.6*A*) and the relative amelioration of VMAT2 LO mice treated with L-DOPA + Tolcapone (repeated measures ANOVA with nested factors, p>0,05; Figure 3.6*D*).

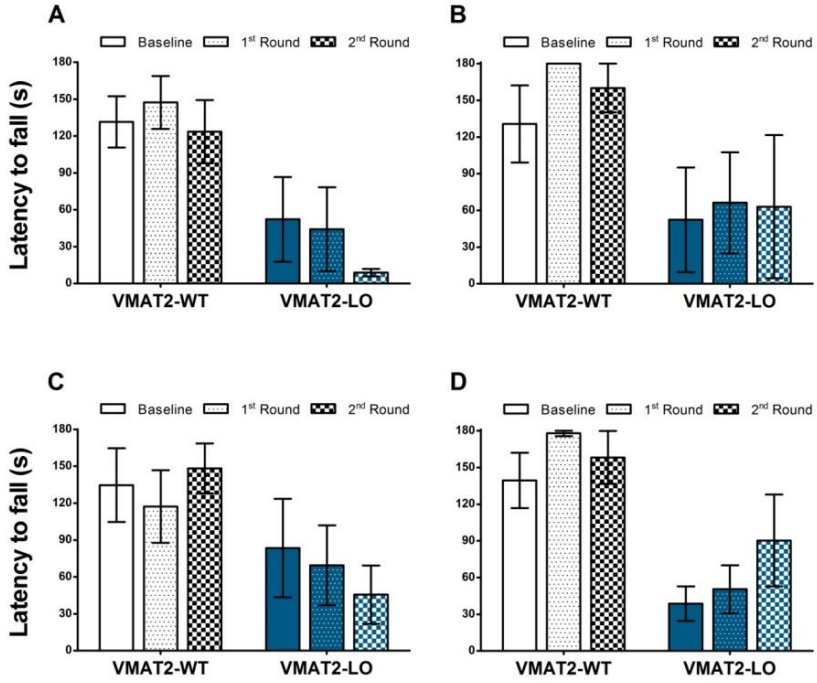

Figure 3.6: The treatments show no significant effect on motor coordination in either genotype over time. VMAT2 WT and VMAT2 LO high

variability can be seen in all the treatments. Results represent the mean latency to fall (s) ± SEM for ***A***, vehicle groups (VMAT2 WT=6, VMAT2 LO=5); ***B***, L-DOPA groups (VMAT2 WT=6, VMAT2 LO=4); ***C***, Tolcapone groups (VMAT2 WT=6, VMAT2 LO=5); ***D***, L-DOPA + Tolcapone groups (VMAT2 WT=6, VMAT2 LO=5).

3.3.3. RIGIDITY OR CATALEPSY

In order to determine the effect of Tolcapone treatments over body rigidity or catalepsy, a bar test (Noain et al., 2013) was conducted as previously described.

The VMAT2 LO mice show a significantly increased spontaneous rigidity at 14 months of age when compared to VMAT2 WT mice (unpaired *t*-test two-tailed, ***p<0,001; Figure 3.7*A*). The phenotypes of either group did not effectively change with the treatments neither at 1st and 2nd rounds of testing (repeated measures ANOVA with nested factors, p>0,05; Figure 3.7*B* and 3.7*C*, respectively).

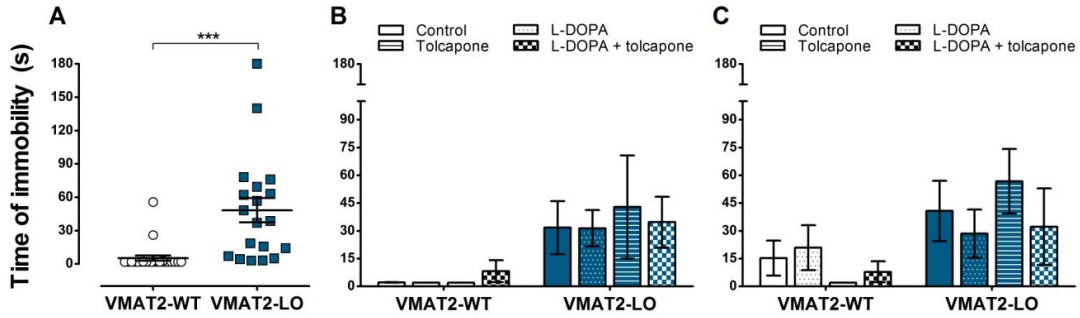

Figure 3.7: VMAT2 LO mice display increased spontaneous rigidity at baseline and do not respond to the interventions at 1st and 2nd rounds. ***A***, VMAT2 LO mice are immobile for longer periods of time in the bar test at 14 months of age. Results represent the mean time of immobility (s) ± SEM per genotype (VMAT2 WT=24, VMAT2 LO=19, ***p<0,001). ***B*** and ***C***, The treatments did not have an effect in any of the groups at 1st and 2nd round, respectively. Results represent the mean time of immobility (s) ± SEM per treatment group (VMAT2 WT: Vehicle=6, L-DOPA=6, Tolcapone=6, L-DOPA + Tolcapone=6; VMAT2 LO: Vehicle=5, L-DOPA=4, Tolcapone=5, L-DOPA + Tolcapone=5).

The evaluation of treatments over time show a significant response in the VMAT2 LO on the L-DOPA + Tolcapone groups between baseline and 2nd round (repeated measures ANOVA with nested factors, *p<0,05; Figure 3.8*D*). A tendency towards worsening of VMAT2 LO mice treated with vehicle can also be appreciated (repeated measures ANOVA with nested factors, p>0,05; Figure 3.8*A*).

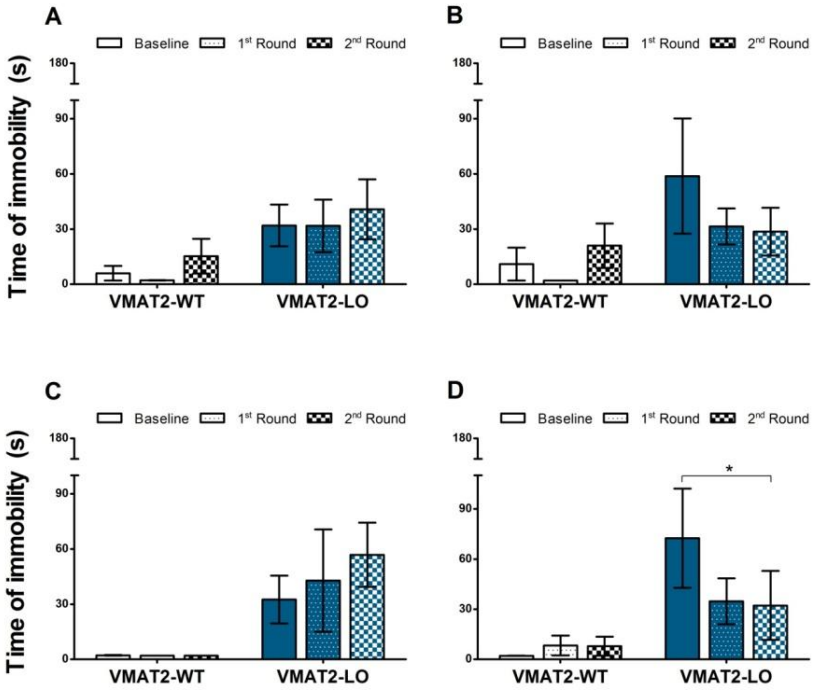

Figure 3.8: The treatments show no significant differences in immobility time in either genotype over time, except in the L-DOPA + Tolcapone group. VMAT2 LO high variability is found in this test in all the treatments. Results represent the mean latency to fall (s) ± SEM for ***A***, vehicle groups (VMAT2 WT=6, VMAT2 LO=5); ***B***, L-DOPA groups (VMAT2 WT=6, VMAT2 LO=4); ***C***, Tolcapone groups (VMAT2 WT=6, VMAT2 LO=5); ***D***, L-DOPA + Tolcapone groups (VMAT2 WT=6, VMAT2 LO=5, **p*<0,05).

3.3.4. OLFACTORY FUNCTION AND EPISODIC MEMORY ASSESSMENT

To test the effect of Tolcapone treatments on olfactory function, an olfactory discrimination test was performed. This test is known not to respond to DA replacement therapy *per se*, thus it was used to evidence the effect of Tolcapone treatment itself (Taylor et al., 2011).

The results show no significant differences at baseline, however the dispersion of the recognition scores is higher in VMAT2 LO mice as compared to VMAT2 WT (unpaired *t*-test two-tailed and one sample *t*-test (to 50%), *p*>0,05; Figure 3.9*A*). Thus, the analysis of treatment effects over unchanged olfactory discrimination becomes irrelevant and is not presented in this thesis.

The novel object recognition test was performed to evaluate the effect of Tolcapone treatments on episodic memory (Büchele et al, 2015).

The results did not show any differences between genotypes at baseline (unpaired *t*-test two-tailed and one sample *t*-test (to 50%), $p>0,05$; Figure 3.9*B*). As before, the analysis of treatment effects over unchanged memory ability becomes irrelevant and is not presented in this thesis.

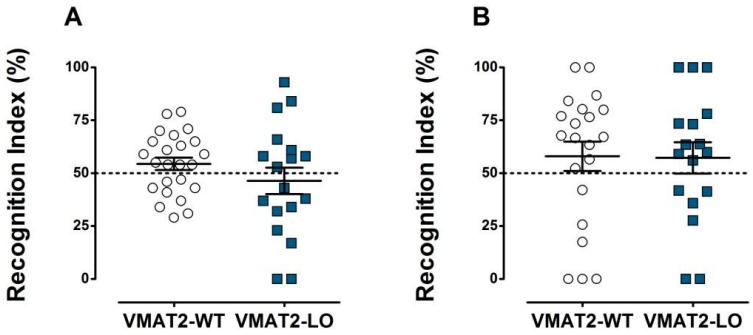

Figure 3.9: VMAT2 WT and VMAT2 LO mice do not display significant differences in olfactory discrimination and novel object recognition at 14 months of age. ***A***, The olfactory discrimination scores of VMAT2 WT and VMAT2 LO mice are not significantly different at 14 months of age. Results represent the mean recognition index (time the animal spent exploring the disc scented with foreign animal's bedding divided per total time the animal spent exploring both discs) ± SEM per genotype (VMAT2 WT=24, VMAT2 LO=18). ***B***, VMAT2 WT and VMAT2 LO mice behave similarly in novel object recognition test at 14 months of age. Results represent the mean recognition index (time the animal spent exploring the novel object divided per total time the animal spent exploring both objects) ± SEM per genotype (VMAT2 WT=21, VMAT2 LO=17).

3.4. QUANTIFICATION OF THCY, ALT AND AST LEVELS

We aim at assessing the tHcy levels in regular blood collections before and after the treatment with Tolcapone, to verify its protective effect on HHcy found in PD patients (Müller and Muhlack, 2009). This analysis will take place in the near future, after all blood samples have been collected and processed.

Since Tolcapone is associated with rare cases of liver damage, the plasma levels of AST and ALT were quantified in VMAT2 WT group treated with vehicle and VMAT2 WT group treated with L-DOPA + Tolcapone, at the end of the 4th round of experiments (unpaired *t*-test two-tailed, $p>0,05$; Figure 3.10*A* and 3.10*B*, respectively). Despite of being slightly decreased on both genotypes comparing to 12 months aged mice (Mazzaccara et al., 2008), the AST/ALT ratio is found to be within standard levels on both genotypes (unpaired *t*-test two-tailed, $p>0,05$; Figure 3.10*C*).

The visual evaluation of the liver at the time of sacrifice and perfusion did not reveal any obvious structural damage (photographic data not shown).

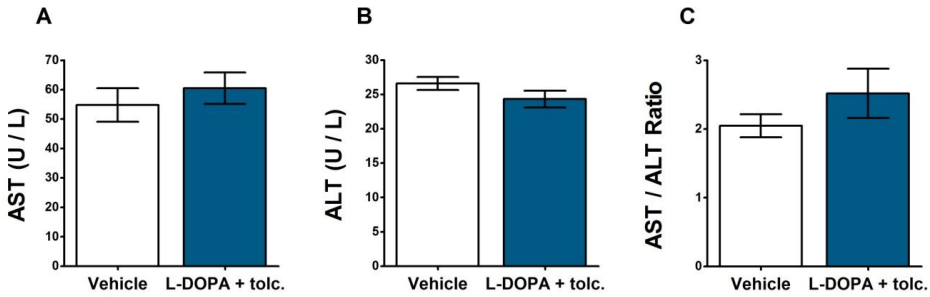

Figure 3.10: Plasma levels of AST and ALT do not show signs of hepatotoxicity related to Tolcapone chronic administration. Plasma levels of AST (***A***) and ALT (***B***) in U/L are within expected levels. Results represent the mean of plasma enzyme ± SEM (VMAT2 WT: Vehicle=4; L-DOPA + Tolcapone=3) ***C***, AST/ALT ratio is marginally increased in the VMAT2 WT group treated with L-DOPA + Tolcapone, yet not reaching concerning levels. Results represent the mean of individual AST/ALT ratios ± SEM (VMAT2 WT vehicle=4, VMAT2 WT L-DOPA + Tolcapone=3).

CHAPTER 4

DISCUSSION AND CONCLUSIONS

Parkinson's disease is a common neurodegenerative disorder afflicting 1-2% of the population aged over 65 and nearly 5% by age 85 (Di Giovanni et al., 2010). With an ageing population, the management of PD is a challenge in clinical practice and research. New mouse models that attempt to fully represent PD are being developed and many of them reproduce, indeed, the complex collection of motor and non-motor features. Regarding the therapeutics, DA replacement stands as the standard treatment for PD although it underlies several complications in the long-term (Stocchi et al., 2008). COMT inhibitors such as Tolcapone have been studied for its efficacy in PD as an adjunctive treatment to L-DOPA, reducing 'off' episodes and possible attenuating the mechanisms linked to vascular events and neurodegeneration (Müller and Muhlack, 2009). In this study, we characterize the motor behaviour of a mouse model of PD with 95% reduced expression of normal VMAT2 protein under L-DOPA and Tolcapone treatment, and attest whether Tolcapone intrinsically acts as autonomous motor ameliorator and vascular and neuronal protector at long term or depends on concomitant use of exogenous L-DOPA in the context of PD.

In order to explore the effects of Tolcapone in motor and non-motor symptoms of PD in VMAT2 LO mice under sub-chronic L-DOPA treatment, an appropriate battery of behavioural tests was designed, including tests responsive and non-responsive to L-DOPA. To distinguish whether Tolcapone had an independent effect on motor features of PD, open field test, rotarod test and bar test were assayed during the '*off*' periods. Moreover, the olfactory discrimination and the novel object recognition tests were performed in the same conditions in order to measure a possible response only linked to Tolcapone in non-motor symptoms either responsive or non-responsive to L-DOPA, respectively.

The motor disabilities in aged VMAT2 LO mice were well characterized by Taylor and colleagues (Taylor et al., 2009). This model displays decreased locomotor behaviour, impaired motor coordination and increased spontaneous rigidity, like our motor tests' results at baseline corroborate. Furthermore, VMAT2 LO have been shown to present increased locomotor activity after acute L-DOPA treatment (Caudle at al., 2007). However, both genotypes do not seem to respond to sub-chronic L-DOPA, Tolcapone or L-DOPA + Tolcapone interventions, with the exception of rigidity or catalepsy, which show amelioration in mutant mice at 14 months old. It is well known that neither L-DOPA nor Tolcapone have a build-up effect that could maintain increased levels of DA during the '*off*' period (Gershanik, 2015). Given that our sub-chronic treatments were interrupted during the testing week, the lack of acute effect of DA replacement was expected. On the other hand, the novel result presented in this thesis is that no disease modifying effect was observed by inhibiting COMT, nor alone or in combination with DA replacement, disregarding rigidity or catalepsy as aforementioned, which suggests some positive influence of COMT inhibition on this symptom's progression.

In the open field test, it is worth to note that all VMAT LO treated groups, except for the vehicle one, seem unable to form a contextual memory –i.e. they lack the expected habituation-to-context effect–, suggesting that the treatments have had a negative impact on memory formation or recall. Further studies would be needed to determine the nature of such observation and explore in more detail possible cognitive disabilities in VMAT2 LO mice. Concerning motor coordination and rigidity, our results show a trend towards a positive effect of L-DOPA therapy, however, animals in the group treated with Tolcapone alone appear not to follow a similar trend. Moreover, it is worth to note the significant impact of L-DOPA + Tolcapone over body rigidity in mutant mice 2 months after the beginning of the treatment. Following studies are needed in these matters.

The non-motor tests assayed in this study show no differences between VMAT2 WT and VMAT LO at baseline. These negative results may relate to several limitations: *a)* the reduced size of the experimental groups, which may have taken power to these results; *b)* both tests were very susceptible to

changes in the environmental conditions such as noise and smells, among others, which may have hampered their sensitivity to detect subtle behavioural changes; *c)* the decreased exploratory behaviour of the VMAT2 LO mice is preponderant in such short trials, evidenced by several subjects not performing the test at all; *d)* the shift between the age of the mice tested in this study and the actual age when the non-motor disturbances are greater, specially dementia; and finally, *e)* the high number of VMAT2 LO different batches over time that were needed to complete the group numbers, which may have had an impact on the variability of the test results.

On the last round of experiments, the feeding behaviour was assessed in order to know whether the significant difference in body weight between genotypes in baseline were due to reduced food intake, owed to damaged reward pathway, or dwarfism, as it has been described in the past for other DA neurotransmission impaired models (Diaz Torga, et al., 2002; Noain et al., 2013). The pharmacologic interventions had no significant effect on body weight progression on both genotypes, but our results suggest that VMAT2 LO mice ingest more than VMAT2 WT ones in relation to their body weight and independently of the treatments. This observation may be linked to a strategy of the mutant animals to compensate for their smaller body weight, or others so far undescribed pathological changes (reduced body temperature, increased metabolism perhaps, etc.). In addition, the power of the VMAT2 LO groups is relatively low. Further analyses with additional data are necessary to confirm these claims. However, our results so far suggest that VMAT2 LO mice have a similar or even increased food intake as compared to their WT controls. Thus, dwarfism becomes a possible explanation for the observed reduced body weight. In detail, hormonal profiling would be needed in order to actually determine a dwarf phenotype in these mice, including determinations of growth hormone among others (Noain et al., 2013).

In regard to the blood markers of hepatotoxicity, which could arise from the heavy drug load over the period of treatment, especially in the groups administrated with Tolcapone, our results show a minor and not significant influence on liver functions between VMAT2 WT untreated and treated with L-DOPA + Tolcapone groups. Further studies on plasma tHcy at

the final endpoint of the pharmacological intervention are planned for the near future.

Overall, our preliminary results suggest that sub-chronic COMT inhibition *per se* or in combination with DA replacement treatment has no or little beneficial effect over motor outcomes in the context of PD. Completion of the 3rd and 4th rounds of testing is needed to appreciate the effect of chronic exposure to the treatment. Furthermore, analysis of tHcy, α-synuclein depositions and loss of midbrain and striatal TH and DAT are planned in order to determine whether COMT inhibition has vascular and neuronal protective properties.

REFERENCES

Avale, Falzone, Gelman, Low, Grandy, Rubinstein (2003) *The dopamine D4 receptor is essential for hyperactivity and impaired behavioral inhibition in a mouse model of attention deficit/hyperactivity disorder*. Molecular Psychiatry Molecular Psychiatry 9: 718–726.

Axelrod J, Tomchick R (1958) *Enzymatic O-methylation of epinephrine and other catechols*. The Journal of Biological Chemistry 233: 702-705

Beal (2001) *Experimental models of parkinson's disease*. Nature Reviews Neuroscience 2:325-334.

Bello, Mateo, Gelman, Noaín, Shin, Low, Alvarez, Lovinger, Rubinstein (2011) *Cocaine supersensitivity and enhanced motivation for reward in mice lacking dopamine D2 autoreceptors*. Nature Neuroscience 14:1033-1038.

Bernheimer H, Birkmayer W, Hornykiewicz O, Jellinger K, Seitelberger F (1973) *Brain dopamine and the syndromes of parkinson and huntington clinical, morphological and neurochemical correlations*. Journal of the Neurological Sciences 20:415-455.

Betarbet R, Sherer TB, Greenamyre JT (2005) *Ubiquitin–proteasome system and parkinson's diseases*. Experimental Neurology 191, Supplement 1:S27.

Binda, M. Milczek, Bonivento, Wang, Mattevi, E. Edmondson (2011) *Lights and shadows on monoamine oxidase inhibition in neuroprotective pharmacological therapies*. Current Topics in Medicinal Chemistry 11:2788-2796.

Björklund A, Dunnett SB (2007) *Dopamine neuron systems in the brain: An update*. Trends in Neurosciences 30:194-202.

Blesa, Phani, Jackson-Lewis, Przedborski (2012) *Classic and new animal models of parkinson's disease*. Journal of Biomedicine and Biotechnology 2012:1-10.

Borges (2005) *Tolcapone in parkinson's disease: Liver toxicity and clinical efficacy*. Expert Opinion on Drug Safety 4:69-73.

Büchele F, Morawska MM, Schreglmann SR, Penner M, Muser M, Baumann CR, Noain D (2015) *Novel rat model of weight drop-induced closed*

diffuse traumatic brain injury compatible with electrophysiological recordings of vigilance states. J Neurotrauma; manuscript in press.

Carlsson A, Falck B, Fuxe K, Hillarp N (1964) *Cellular localization of monoamines in the spinal cord*. Acta Physiologica Scandinavica 60:112–119.

Cartier, Parra, Baust, Quiroz, Salazar, Faundez, Egana, Torres (2009) *A biochemical and functional protein complex involving dopamine synthesis and transport into synaptic vesicles*. Journal of Biological Chemistry 285:1957-1966.

Caudle, Richardson, Wang, Taylor, Guillot, McCormack, Colebrooke, Di Monte, Emson, Miller (2007) *Reduced vesicular storage of dopamine causes progressive nigrostriatal neurodegeneration*. Journal of Neuroscience 27:8138-8148.

Chaudhry, Edwards, Fonnum (2008) *Vesicular neurotransmitter transporters as targets for endogenous and exogenous toxic substances*. Annual Review of Pharmacology and Toxicology 48:277-301.

Chaudhuri KR, Healy DG, Schapira AH (2006) *Non-motor symptoms of parkinson's disease: Diagnosis and management*. The Lancet Neurology 5:235-245.

Comella (2007) *Sleep disorders in parkinson's disease: An overview*. Movement Disorders 22:S367-S373.

Daubner, Le, Wang (2011) *Tyrosine hydroxylase and regulation of dopamine synthesis*. Archives of Biochemistry and Biophysics 508:1-12.

Deane K, Spieker S, Clarke CE (2004) *Catechol-O-methyltransferase inhibitors for levodopa-induced complications in parkinson's disease*. Cochrane Database Syst Rev*:CD004554*.

Di Giovanni, Eleuteri, Paleologou, Yin, Zweckstetter, Carrupt, Lashuel (2010) *Entacapone and tolcapone, two catechol O-methyltransferase inhibitors, block fibril formation of -synuclein and -amyloid and protect against amyloid-induced toxicity*. Journal of Biological Chemistry 285:14941-14954.

Díaz-Torga, Feierstein, Libertun, Gelman, Kelly, Low, Rubinstein, Becú-Villalobos (2002) *Disruption of the D2 dopamine receptor alters GH and IGF-I secretion and causes dwarfism in male mice*. Endocrinology 143:1270-1279.

Ehringer H, Hornykiewicz O (1998) *Distribution of noradrenaline and dopamine (3-hydroxytyramine) in the human brain and their behavior in diseases of the extrapyramidal system1*. Parkinsonism & Related Disorders 4:53-57.

Erickson JD, Schafer MK, Bonner TI, Eiden LE, Weihe E (1996) *Distinct pharmacological properties and distribution in neurons and endocrine cells of two isoforms of the human vesicular monoamine transporter*. Proc Natl Acad Sci USA *93(10): 5166–5171* .

Espinoza, Manago, Leo, D. Sotnikova, R. Gainetdinov (2012) *Role of catechol-O-methyltransferase (COMT)-dependent processes in parkinson's disease and L-DOPA treatment*. CNS & Neurological Disorders - Drug Targets 11:251-263.

Falck B, Hillarp N-, Thieme G, Torp A (1982) *Fluorescence of catechol amines and related compounds condensed with formaldehyde*. Brain Res Bull 9(1-6):xi-xv.

Fearnley JM, Lees AJ (1991) *Ageing and parkinson's disease: Substancia nigra regional selectivity*. Brain 114 (Pt 5):2283-301.

Forno LS (1996) *Neuropathology of parkinson's disease*. Journal of Neuropathology & Experimental Neurology 55(3):259-272.

Gershanik (2015) *Improving L-DOPA therapy: The development of enzyme inhibitors*. Movement Disorders 30:103-113.

Gilks WP, Abou-Sleiman PM, Gandhi S, Jain S, Singleton A, Lees AJ, Shaw K, Bhatia KP, Bonifati V, Quinn NP, Lynch J, Healy DG, Holton JL, Revesz T, Wood NW (2005) A *common LRRK2 mutation in idiopathic parkinson's disease*. The Lancet 365:415-416.

Giros, Jaber, Jones, Wightman, Caron (1996) *Hyperlocomotion and indifference to cocaine and amphetamine in mice lacking the dopamine transporter*. Nature 379:606-612.

Goedert (2001) *Alpha-synuclein and neurodegenerative diseases*. Nature Reviews Neuroscience 2:492-501.

Guillot, Miller (2009) *Protective actions of the vesicular monoamine transporter 2 (VMAT2) in monoaminergic neurons*. Molecular Neurobiology 39:149-170.

Guo, Chen, Kong, Zhu, Ma, Qin (2007) *Inhibition of vesicular monoamine transporter-2 activity in α-synuclein stably transfected SH-SY5Y cells*. Cellular and Molecular Neurobiology 28:35-47.

Jankovic (2008) *Parkinson's disease: Clinical features and diagnosis*. Journal of Neurology, Neurosurgery & Psychiatry 79:368-376.

Jones SR, Gainetdinov RR, Jaber M, Giros B, Wightman RM, Caron MG (1997) *Profound neuronal plasticity in response to inactivation of the dopamine transporter*. Proc Natl Acad Sci USA 95(7): 4029–4034.

Klein, Westenberger (2012) *Genetics of parkinson's disease*. Cold Spring Harbor Perspectives in Medicine 2(1):a008888.

Kuhar MJ (1992) *Molecular pharmacology of cocaine: A dopamine hypothesis and its implications*. Ciba Foundation Symposium 166:81-89; discussion 89.

Langston JW (2006) *The parkinson's complex: Parkinsonism is just the tip of the iceberg*. Annals of Neurology 59:591–596.

Larson (2014) *Deep brain stimulation for movement disorders*. Neurotherapeutics 11:465-474.

Leegwater-Kim, Waters (2006) *Tolcapone in the management of parkinson's disease*. Expert Opinion on Pharmacotherapy 7:2263-2270.

Li L, Chin L- (2003) *The molecular machinery of synaptic vesicle exocytosis*. CMLS, Cell Mol Life Sci 60:942-960.

Little S, Brown P (2014) *Focusing brain therapeutic interventions in space and time for parkinson's disease*. Current Biology 24:R909.

Lotharius, Brundin (2002) *Pathogenesis of parkinson's disease: Dopamine, vesicles and α-synuclein*. Nature Reviews Neuroscience 3:932-942.

Mazzaccara, Labruna, Cito, Scarfò, De Felice, Pastore, Sacchetti, Blagosklonny (2008) *Age-related reference intervals of the main biochemical and hematological parameters in C57BL/6J, 129SV/EV and C3H/HeJ mouse strains*. PLoS ONE 3:e3772.

McNaught, Olanow, Halliwell, Isacson, Jenner (2001) *Failure of the ubiquitin–proteasome system in parkinson's disease*. Nature Reviews Neuroscience 2:589-594.

Missale C, Nash SR, Robinson SW, Jaber M, Caron MG (1998) *Dopamine receptors: From structure to function*. Physiol Rev 78(1):189-225.

Mooslehner, Chan, Xu, Liu, Smadja, Humby, Allen, Wilkinson, Emson (2001) *Mice with very low expression of the vesicular monoamine transporter 2 gene survive into adulthood: Potential mouse model for parkinsonism*. Molecular and Cellular Biology 21:5321-5331.

Müller, Muhlack (2009) *Peripheral COMT inhibition prevents levodopa associated homocysteine increase*. Journal of Neural Transmission 116:1253-1256.

Müller, Kuhn (2006) *Tolcapone decreases plasma levels of S-adenosyl-L-homocysteine and homocysteine in treated parkinson's disease patients*. European Journal of Clinical Pharmacology 62:447-450.

Noain, Perez-Millan, Bello, Luque, Casas Cordero, Gelman, Peper, Tornadu, Low, Becu-Villalobos, Rubinstein (2013) *Central dopamine D2 receptors regulate growth-hormone-dependent body growth and pheromone signaling to conspecific males*. Journal of Neuroscience 33:5834-5842.

Pan, Kondo, Le, Jankovic (2008) *The role of autophagy-lysosome pathway in neurodegeneration associated with parkinson's disease.* Brain 131:1969-1978.

Parkinson (2002) *An essay on the shaking palsy.* The Journal of Neuropsychiatry and Clinical Neurosciences 14:223-236.

Pfeiffer RF (2003) *Gastrointestinal dysfunction in parkinson's disease.* The Lancet Neurology 2:107-116.

Postuma, Lang (2004) *Homocysteine and levodopa: Should parkinson disease patients receive preventative therapy?* Neurology 63:886-891.

Saavedra, Baltazar, Duarte (2008) *Driving GDNF expression: The green and the red traffic lights.* Progress in Neurobiology 86:186-215.

Saito M, Maruyama M, Ikeuchi K, Kondo H, Ishikawa A, Yuasa T, Tsuji S (2000) *Autosomal recessive juvenile parkinsonism.* Brain and Development 22, Supplement 1:115-117.

Schapira AH (2008) *Mitochondria in the aetiology and pathogenesis of parkinson's disease.* The Lancet Neurology 7:97-109.

Stocchi F, Tagliati M, Olanow CW (2008) *Treatment of levodopa-induced motor complications.* Movement Disorders 23:S599–S612.

Sun, Li, Yang, Yu, Wu, Li (2014) *Exposure to atrazine during gestation and lactation periods: Toxicity effects on dopaminergic neurons in offspring by downregulation of Nurr1 and VMAT2.* International Journal of Molecular Sciences 15:2811-2825.

Takahashi N, Miner LL, Sora I, Ujike H, Revay RS, Kostic V, Jackson-Lewis V, Przedborski S, Uhl GR (1997) *VMAT2 knockout mice: Heterozygotes display reduced amphetamine-conditioned reward, enhanced amphetamine locomotion, and enhanced MPTP toxicity.* Proceedings of the National Academy of Sciences 94:9938-9943.

Taylor, Caudle, Miller (2011) *VMAT2-deficient mice display nigral and extranigral pathology and motor and nonmotor symptoms of parkinson's disease.* Parkinson's Disease 2011:1-9.

Taylor, Caudle, Shepherd, Noorian, Jackson, Iuvone, Weinshenker, Greene, Miller (2009) *Nonmotor symptoms of parkinson's disease revealed in an animal model with reduced monoamine storage capacity.* Journal of Neuroscience 29:8103-8113.

Voon V, Fox SH (2007) *Medication-related impulse control and repetitive behaviors in parkinson disease.* Arch Neurol 64:1089-1096.

Warner TT, Schapira AHV (2003) *Genetic and environmental factors in the cause of parkinson's disease.* Annals of Neurology 53:S16–S25.

Wayment HK, Schenk JO, Sorg BA (2001) *Characterization of extracellular dopamine clearance in the medial prefrontal cortex: Role of monoamine uptake and monoamine oxidase inhibition.* J Neuroscience 21(1):35-44.

Zhou Q, Quaife CJ, Palmiter RD (1995) *Targeted disruption of the tyrosine hydroxylase gene reveals that catecholamines are required for mouse fetal development.* Nature 374:640-643.

Ziemssen T, Reichmann H (2007) *Non-motor dysfunction in parkinson's disease.* Parkinsonism & Related Disorders 13:323-332.